ABOVE AND BELOW GROUND PHENOTYPING METHODS FOR CORN

BY

WILLIAM E. ROY

THESIS

Submitted in partial fulfillment of the requirements
for the degree of Master of Science in Technical Systems Management
in the Graduate College of the
University of Illinois at Urbana-Champaign, 2013

Urbana, Illinois

Adviser:
        Associate Professor Tony E. Grift

ABSTRACT

Over the past few decades, both researchers and commercial farmers have attempted to find means to accurately predict crop yields during the growing season. Modern science has been successful in mapping the genes of crops to help aid in drought protection, germination timing, and frost protection. These biological traits have assured crop seed strength and protection, enabling higher yields. However, many other physical traits such as plant height, leaflet count, color, germination rate, and biomass are indicators of the plants' overall health and future yields.

This research provided a means in which an operator can measure an individual trait of a corn plant, and predict yield. The first study used an imaging system comprising a CCD camera and a slanted laser sheet, to measure the diameter of the corn stalk. After processing the data, the diameters of the corn stalks were shown to be positively correlated with the grain weight of the corn ear. Therefore, the system allows the farmer to predict the per-plant-yield (PPY) based on measuring the diameters of the corn stalks. In addition, the measurement system is easy to use, and is not affected by environmental conditions such as ambient light. The accuracy of the optical system was determined by comparing the measurements against those taken with a pair of digital calipers. 26.7 and 33.5 mm PVC tubes were used to assess the measurement accuracy. The optical system measured the diameter of the PVC tubes with an accuracy of 98% while varying the location of the PVC tubes within the measurement zone. The same optical system was used in the greenhouse to measure diameters of corn stalks, where the accuracy decreased to 84% due to measurement location variability created by the corn stalks.

The theme of phenotyping was extended in the second part of the research. While the corn stalk data could be used to predict the PPY, the below ground root system is indicative of

the plants' stability, and of its ability to reach nutrients and water. A "Rhizotron" was constructed, which consists of a soil volume, visible behind a vertical glass pane. By growing a single corn plant in the Rhizotron, its roots are being pushed against the glass pane which allows for studying root development over time. A key parameter is the root angle, which has been shown highly influential in explaining the historic yield increases in the Midwest over the past decades (Hammer, et al., 2002). Since the roots grow behind a glass pane, the challenge was to obtain high resolution images of the root systems without reflections created on the glass. A camera was mounted on a linear actuator that allowed for taking images that can be overlapped to produce a complete mosaic of the root system.

DEDICATION

I would like to dedicate this work to my parents. They taught me at an early age to always want more from myself and to gain the most from my education. With their unwavering support both financially and emotionally, I was always able to focus on my work and have the opportunities to achieve the best results. They had shown me that with better education come better rewards.

ACKNOWLEDGMENTS

TABLE OF CONTENTS

List of Abbreviations

AGP   :   above ground plant

BGP   :   below ground plant

CCD   :   charge coupled device

HTPP   :   high throughput plant phenotyping

ILS   :   illuminated line segment

PPY   :   per-plant-yield

QTL   :   quantitative trait loci

RIL   :   recombinant inbred lines

1   INTRODUCTION

The prime goal of any production agriculture enterprise is to produce a high crop yield, at the lowest possible cost, while minimizing environmental impact. Farmers have adapted various practices and technologies to maintain the fertility, performance, and profitability of their crops and fields. For instance, Variable Rate Application (VRA) has been used to properly disperse crop-care chemicals at a prescribed rate. More recently, bioengineering has been adopted to create a healthier, and a more robust crop. Because of genomic research, crop seeds incorporate controlled germination, drought resistance, and even resistance to weed control chemicals. Corn yields have increased steadily over time, mainly owing to the development of hybrid seeds (see figure 1).
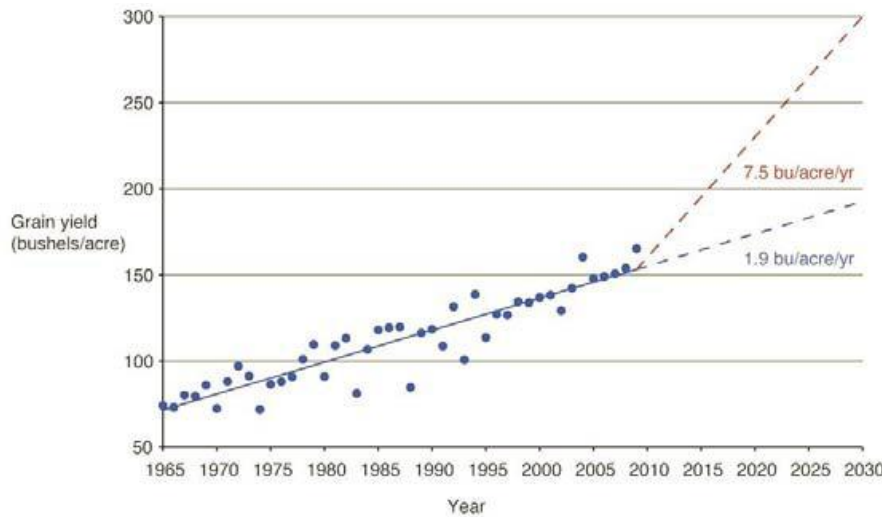
Figure 1: Historical trends in corn yield (University of Nebraska at Lincoln)

Represented by the blue line in figure 1, from 1965 to 2010 grain yields have been increasing mainly due to the development of hybrid corn varieties. However to feed the projected world population in 2030, the current increase of 1.9 bushel/acre/year must be improved to an

annual increase of 7.5 bushel/acre/year. Since the globally available farmland is not expected to

increase, plants will have to be planted closer together to increase yield per area. Newer hybrid

corn plants allow this, since they exhibit leaves that are more vertical, a feature that is mimicked

in the root system. In other words, modern corn hybrids can be planted closer together while

maintaining the PPY potential, which increases the yield per unit of area.
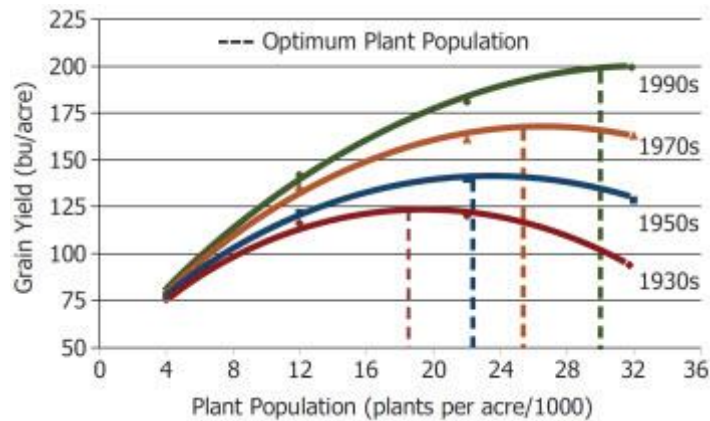
Figure 2: Graph of increasing yield with respect to plant population over the last 60 years
(Duvick, 2005)

However, figure 2 shows the existence of an optimum value for plant population, since

planting more seeds per area may increase total yield up to a point where the PPY decreases due

to interplant competition for light and nutrients (Wiley & Heath, 1969). Measuring the yield of a

field at harvesting time is standard practice using yield monitors, but a practical research tool that

predicts the PPY during the growing season is not available. Such a tool was developed which

operates on the principle of measuring the diameters of corn stalks as a proxy for PPY. The

requirements of the tool were the ability to accurately measure corn stalk diameters, simplicity of

operation, and robustness under field conditions.

In addition to the need of for above ground phenotyping tools, below ground tools are

equally scant. Corn root systems develop in relation to soil, which is a complex amalgamation of

sand, silt and clay, composing aggregates separated by pores that conduct water flows. Tillage is

performed to achieve optimal soil conditions for emergence and growth. To study root structure

development in relation to soil, water and nutrient parameters, and a visualization tool is key.

The Rhizotron is such a tool, in which roots are allowed to grow against a transparent surface

through which they can be observed (Huck & Taylor, 1982). An example is shown in figure 3

where the transition from Illinois Drummer soil to a clay soil is visible. The number of root

branches and root hairs dictate the amount of water the plant can collect from the soil. Note the

response of the root structure to the varying aggregate size between the two soils.

Figure 3: Rhizotron image of a root system. Note the adaption of the roots to the change from
Drummer soil (top) to clay (bottom).

Human interpretation of the root system is prone to inaccuracy and inconsistency while

lacking records of the data. Therefore, instead of human observation, a machine vision system is

needed that can record the root growth behind a glass pane (see figure 3). Initial attempts in Australia used a high-resolution flat-bed scanner to obtain images, but this method is destined to fail, since the imaging of objects behind glass (such as portraits) requires that the light introduced is not reflected directly into the imaging sensor. Alternatively, a system was devised in which reflections were eliminated by placing a camera behind a non-reflective surface, and by introducing light laterally. In addition, a method was developed in which images are taken automatically, and overlapped to form a mosaic of the complete Rhizotron. These high-resolution images will allow researchers to study the development of the root system, and to apply algorithms to measure root parameters, which can be related to the plant's genotyping and growing conditions.

The objective of the first part of this research was to determine the relationship between semi-automatically measured corn stalk diameters and PPY. The measurement platform consisted of a digital camera combined with a slanted laser sheet, and was termed the "Corn Cane". By observing the "illuminated line segment" (ILS) sheet as projected onto a corn stalk, the diameter was measured. A complete description of the principle can be found in (Zhang & Grift, 2012).

The objective of the second part of the research was to develop a machine vision system that generates high-resolution images of corn growing behind a reflective transparent surface.

1.1   Summary of Results

The Corn Cane proved capable of measuring the diameter of the corn stalks and providing the data showing a strong correlation between the corn stalk diameter and PPY. The Rhizotron yielded reflection-free images of roots growing behind a glass pane, demonstrating its feasibility as a tool for root research.

1.1.1 Corn stalk measurement system results

The Corn Cane was able to measure the diameters of PVC tubes in the laboratory with an accuracy of 98%. In the greenhouse, the stalk diameters of corn plants were measured with an accuracy of 84%, the reduction in accuracy between PVC tubes and corn stalks stems from the discrepancy between the interaction of the caliper and the Corn Cane with the poorly defined natural stalks. A positive correlation was determined between stalk diameter and PPY ($R2 = 0.762$). This proves the feasibility of the Corn Cane and a PPY prediction tool.

1.1.2 Rhizotron imaging system results

The Rhizotron imaging system was able to acquire detailed imagery regarding root structures behind a glass screen. A semi-automated system was implemented that acquired images with sufficient overlap to allow composing a mosaic of the whole Rhizotron surface. One of the limiting factors was the emergence of algae behind the glass surface that limited the imaging process. This phenomenon must be avoided in future experiments.

2   LITERATURE REVIEW

The Phenotype of a plant is the physical expression of its underlying genotype, in addition to its growth environment. Plant phenotyping is the measurement of plant characteristics (traits) such as yield (as in this research). Other traits of interest in production agriculture comprise nutrient and/or water uptake, response to biotic stress such as to insect attacks, diseases or response to abiotic stresses such as drought. The phenotyping measurements are often done manually, but technology can aid in accelerating this process as well as potentially improving the quality of the measurements. Many automatic phenotyping methods rely on inexpensive cameras and computing power. This practice leads to repositories of digital images of many plant traits over long periods. The images are analyzed to extract pertinent information from the measurement (Grift, Bohn, & Novais, 2011). The growing image repositories gradually form a comprehensive dataset potentially explaining how plants grow function in a given environment (Eberius & Lima-Guerra, 2009). High-throughput plant phenotyping (HTPP) data can also be used in crop breeding, where a measured trait (for instance yield) among many plants with known genotypes is used to identify regions in the plant's genome that have an influence on that particular trait. These measured traits can be used to create quantitative trait loci (QTL) maps that may explain plant productivity (yield, water use, and nitrogen capture), in comparison to their root structures and environmental conditions (de Dorlodot, et al., 2007).

2.1   Above ground phenotyping

Phenotyping methods can explain plant development and their traits related to growth. These traits can be seen through plant height, area, or volume of different parameters important to plant functions. The functions such as canopy density, plant transpiration via plant leaf area, and water uptake and root strength can change for each species of plant (Tang & Boyer, 2002). While each

physical trait is unique to the individual genotype of corn, sensitivities of leaf growth to temperature, soil water status or evaporative demand can be reproducible throughout different species (Parant & Tardieu, 2012). In an attempt to transfer the trait of expanded leave elongation in corn (Dignat, et al., 2012), created a global study to QTL map the leaf elongation rate (LER_{max}) of 5 recombinant inbred lines (RIL) of corn from tropical and dry world locations. Due to the scale of the study the QTLs co-location is a powerful tool to test the similarity of genetic controls between multiple traits (El-Lithy, et al., 2010). Within an outdoor experiment and greenhouse study, 76 prominent trait lines were crossbred into the B37 corn strain. Progress was established by measuring the corn leave area with rulers of the 6th and 8th leaf during growth. Growth was not promoted in an excessive manner outside of common standards. Fertilizer, water, and lighting times remained constant and each RIL received the same amount of attention. The study had a large impact on high throughput phenotyping by demonstrating in all 5 global locations LER_{max} traits identified through QTLs can be transferred to other species of corn.

Drought resistance, plant height, and plant temperature are all controlled by plant physiology. During drought conditions, corn leaf stomata reduce their leaf pore openings in attempts to conserve water. This decrease in stomatal conductance also leads to the reduction in plant height and yields (Payero, et al., 2009). Once the stomata reduce in size, the plant canopy increases in temperature compared to plants not under stress. Drought resistant corn strains can be identified through the relationship of thermal imaging, height measurement, and plant moisture content and detect the genetic differences through phenotyping a large number of genotypes under water-deficit conditions (Munns, et al., 2010). In a large field experiment, to track these genetic traits of drought resistance (Zia, et al., 2013) planted 300 single cross hybrids in a well-watered field located in Morelos Mexico. The study was split into 6 sections of mature

plants and young plants. Each section had well watered, and watered stressed plants. The 3 water stressed plots were subjected to drought conditions. The purpose of the research was to1) phenotype the plant height and canopy temperature through thermal imaging to ascertain the status of the leaf stomata 2) Note if any of the single cross hybrids exhibit or not exhibit signs of water stress. The outcome with the study concluded that for each day of water removal canopy temperatures increased 4° Celsius due to stomata reducing their size in water stressed plants, however only 1° Celsius for the canopy leaves of well watered plants. Height of the younger plants was stunted by 35% while in mature plants height changes were not noticed. The plants most negatively affected were noted to range from (young – blister). Final yield was reduced 60% for all water stressed plants when compared to well water plant yields. The physiological and phenotypic characteristics of corn leaf temperature response to water stress indicated a significant relationship to yield.

2.2   Below ground phenotyping

There are several methods to ascertain the genetic information of plants from above ground phenotyping (AGP) however the soil contains comparatively the same amount of plant information (Lobet & Draye, 2013). Root growth is essential to the overall plant performance, and attempts have been made to observe root structures over time dating back to the early 1900s (McDougall, 1916) . These early attempts to measure the root structures were conducted by hand and were time consuming. Handheld measuring enabled for a large potential of error due to the conventional (of the time) methods of record keeping ascertaining to the physical parameters of the root structures (Calfee, 2003). Presently, Rhizotrons are becoming utilized and are devices for non-destructive below ground phenotyping (BGP) of plant roots over time. The Rhizotron enables researchers to clearly view the root development progress and the soil conditions of

plants without having to remove or transplant the plants into different vessels post phenotype (Garrigues, et al., 2006). While Rhizotrons allow for BGP, root complications arise from inherent environmental obstructions that weaken the ability to emulate true growing conditions caused by some Rhizotrons physical structures. Due to the sizes of root structures, the small volume of soil within the Rhizotron severely reduces the root architecture, forming unnatural root arrangements (Ugoji & Laing, 2008). Updated methods to improve the conditions of the root environments have are been implemented to collect accurate root poses. The poses are characterized by the measurements of root angles at the axes of predominant roots, the diameter of the roots, and the root overlap of different root orders. Rhizotron root data collection has been accomplished in two forms: *in-situ,* where the descriptions and measurements of the roots are formed by outside imaging through the viewing window or through trace drawings of the viewable root structures, *ex-situ*, the less common method of removing the total plant and root structures from the Rhizotron and scanning the root body in a laboratory (Mooney, et al., 2011).

To combine both methods of data extraction (Lobet & Draye, 2013) constructed several small Rhizotrons to grow twenty maize plants of the B73 genotype. The method of research was to scan the entirety of the root body within the Rhizotron to measure the root architecture after 20 days of growth. The anticipated outcomes of these scans were to produce vectorized root system images of genotype B73 and to determine if the genotype developed proper root angles and root structure densities enabled for maximum water uptake. The conclusions were that the root scanning method produced images that when compared to *ex-situ* images were 98% accurate and in both phenotyping methods genotype B73 produced root systems of adequate densities for proper water uptake. However, the study was limited by the physical size of the Rhizotron and growing media provided for the maize. The Rhizotron being narrow bodied did not allow for the

roots to elongate in all 3 dimensions as per environmental conditions, and the growth media contained greater concentrations of sand uncommon to maize growing condition.   Common growing conditions for maize allow the root systems to react to stimuli in a more natural manner as found in proper soil condiditons. When corn roots are not subjected to grow in an unnatural manner, the relationship between root elongation and root diameter can reveal important clues as to the growth rates of different root types (Hackett & Rose, 1972). (Cahn, et al., 1989), allowed 5 maize plants to grow and develop in Rhizotrons consisting of soil with parameters consistent to New York maize. Within the the Rhizotrons, the relationship of root elongation to root diameter were phenotyped *in-situ* by hand and not electronic devices. The conclusions of this study were with the maize seed (Zea mays L. cv. Cornell 175), the correlation was positive for the first 60 days of growth. After 60 days the root structures maintained current root size. However again with current Rhizotron body designs the narrow body the roots while in correct growing media, were subjected to two dimensional growth.

Corn root growth can become negatively influenced the the soild bulk density of the soil in which the seeds are planted. Generally, root growth rates decrease with the increase of soil bulk density, however the ratio varies dramatically depending on the soil types and seeds planted (Wolkowski, 1991). The reason being for decreased rates of growth in corn are attributed to specific corn root structures' ability to uptake water and nutrients become restricted due to slow root growth (Kooistra, et al., 1992). To better understand which hybrids of Zea mays L. cv. Pioneer 3325 seeds could with stand increasing soil compactions, and continue to promote root growth (Kuchenbuch & Ingram, 2004), constructed Rhizotrons with loamy sand soil ranging from 1.25 g cm^{-3} to 1.66 g cm^{-3} to measure the progress of root growth progress of the hybrids in increasing soil bulk densities. All measurments were conducted by hand, indicating the Zea mays

L. cv. Pioneer 3325 seeds suffered a total growth reduction of 30% and the seminal roots as expected suffered exponential biomass reduction with the root structures further progressing into the compacted soil of the Rhizotron. The noted progress of the hydbrid seeds yield the assumption that with a heterogeneous soil mix, roots with larger diamaters than the pore space they occupy must become thinner or displace the soil particles to remain the same size with respect to growth and nutriant uptake (Goodman & Ennos, 1999) .

2.3   Literature review synopsis

Methods to clearly identify traits of the corn plant have been implemented throughout the last century. ABP is the process in which phenotypic traits located at the soil height or higher are referenced to specific genotypes. Current research utilizes both hand measurement and electronic measurement such as cameras, computers, and infrared imaging, depending on the phenotype method application. Traits such as growth, leaf size, drought resistance, and plant transpiration can be identified and exploited to other species of plant if the genetic cause for these phenotypes is located and exploited. Trait transfer can be accomplished through crossbreeding either in a controlled field environment or the laboratory.

BGP is the extraction of phenotypic information of corn plants below the soil line. The most focused on aspect of research is the root and root architecture. Early methods included extraction of roots thus damaging the roots. Later methods have been attempted to clearly view and image root bodies through the use of Rhizotrons. Currently, Rhizotrons are limited by their volumetric size in which the corn plant is housed. The growing media is chosen between aggregates of soil, sand, and other growing media that allow for proper imaging however, produce unrealistic root geometry such as gels. Rhizotrons that allow for proper root development and total imaging with the use of soil have to extract data *ex-situ* making repetition with the same plant difficult.

3 MATERIALS AND METHODS

In this research, two devices were developed, aimed at above and below ground phenotyping of corn plants respectively. The above ground instrument was termed the "Corn Cane", a handheld device aimed at measuring corn stalk diameters under field conditions. The below ground instrument is typically termed a Rhizotron, and its purpose is to visualize the development process of plant roots.

3.1 Above ground phenotyping

The objective of above ground phenotyping was to produce a system capable of measuring the diameters of corn stalks as a proxy for PPY, in a high-throughput manner (see figure 4).
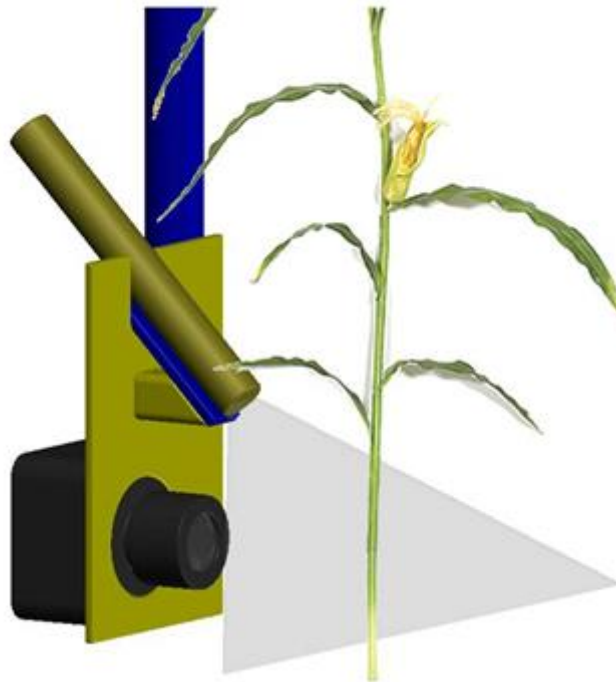

Figure 4: CAD rendering of the Corn Cane

The development of the corn stalk measurement system required the following activities:

1. Construct a platform to carry the sensing system/camera and laser sheet.

2. Calibrate the imaging system using standardized procedures.

3. Determine the imaging system accuracy using objects with constant diameters.

4. Test the imaging system outdoors to determine the sensitivity to ambient lighting conditions.

5. Set up a winter greenhouse experiment with soil nutrients and environmental conditions representing the Midwest.

6. Conduct regression analysis to determine the relationship between manually measured stalk diameters and measured stalk diameter using the imaging system.

7. Conduct regression analysis to determine the relationship between measured diameters (using the imaging system) stalk diameters and PPY.

The concept of corn stalk diameter measurement was based on the use of a machine vision system comprising a single camera (Unibrain® Fire-i 701c), and structured lighting. The structured lighting was provided by projecting a laser beam through a Fresnel lens which created a laser sheet. This laser sheet was slanted downward at a 45 degree angle and projected onto a corn stalk, which resulted in a crescent-shaped illuminated line segment (ILS) that was observed by the camera. The location of the ILS in the image allowed for determination of the distance from the stalk to the camera's Charge Coupled Device (CCD) chip. This distance was used to translate the measured width of the ILS into a stalk diameter.

To make the ILS clearly visible and distinguishable from the background, in the laboratory the idea of image subtraction was pursued. Here, one image is acquired with and another without the laser sheet lighting. Under the assumption that the image scene remains constant during the imaging process, subtracting the images theoretically results in a difference image in which the ILS is prominent. The subtraction method worked well in the laboratory, but during field trials the assumption of a constant imaging scene was impossible to justify, resulting in excessive imaging noise. Therefore, during field trials this method was replaced by an alternative where the

ILS presentation was enhanced using a bandpass filter (Edmund Optics ® 65-700), matched to the wavelength of the laser sheet (532 nm). This method also required changing the triggering mechanism, which in the subtraction method was implemented by external activation of the laser through a data acquisition module (National Instruments, NI 6009). In the final version, the camera was continuously acquiring images at a rate of 15 frames per second, and when a segmented image contained more than 500 white pixels (caused by the ILS on a stalk) the image was saved. The number of 500 was determined through experimentation.

3.1.1   Corn Cane camera calibration

Camera calibration is a necessary step to ensure diameter measurement accuracy. Here, the camera's intrinsic and extrinsic parameters were identified to be used later in the Matlab® scripts for image analysis. Intrinsic parameters are unique to the camera, whereas extrinsic parameters are distortion coefficients which are a function of the lens. The complete works of the camera calibration process for Matlab® can be found on California Institute of Technology: (Bouguet & Jean-Yves, 2010).
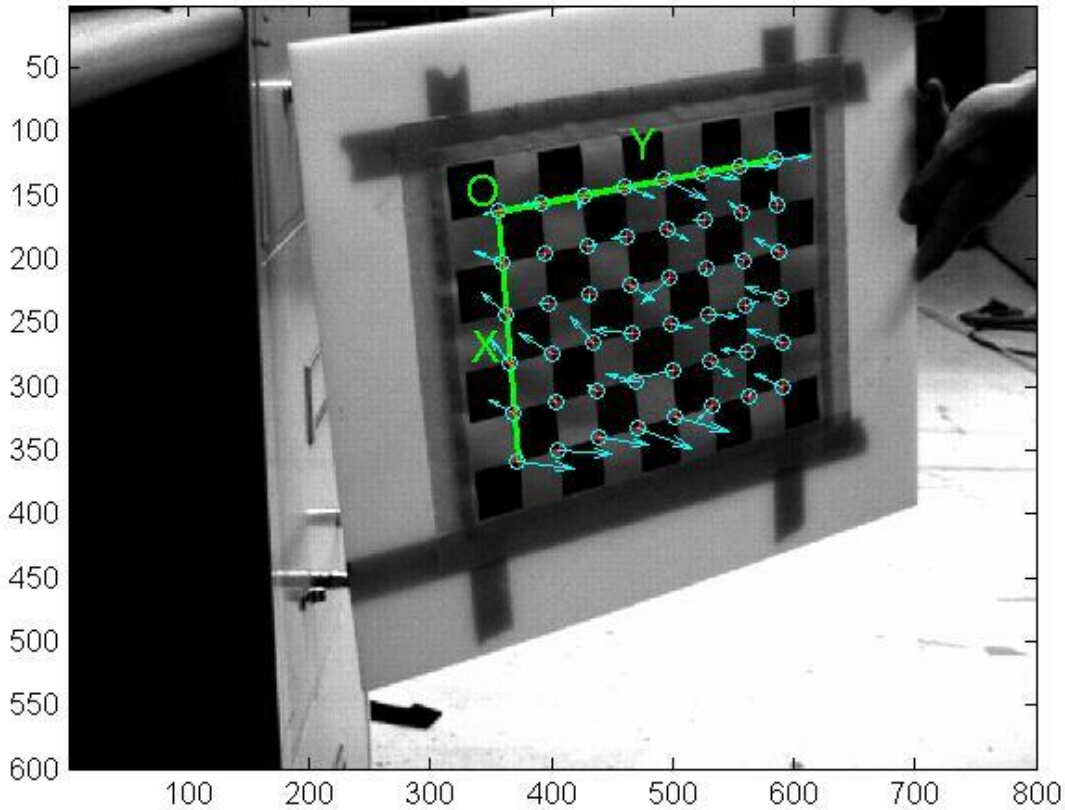
Figure 5: Corner extraction calibration method to identify intrinsic parameters

A target board containing checkered grids was used for calibration. The first step was to establish a common origin that could be identified in all calibration images. By creating a boundary grid from selected corners, the Matlab® Image Acquisition Toolbox was able to identify the pitch and skew of the target board (see figure 5). Upon completion of corner extraction, the parameters of the camera and lens could be identified. Once these parameters were identified, calibration constants were computed that were used in the remaining machine vision tasks.
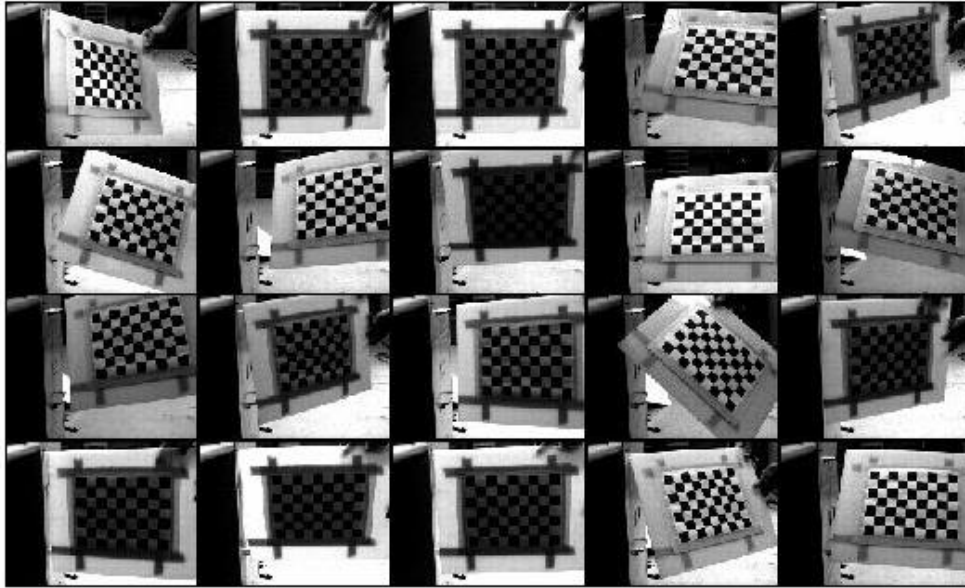
Figure 6: All 24 calibration images used in corner extraction

All 24 images were analyzed in the same manner (see figure 6). The common origin was established to be the top left of each image. For proper calibration, sufficient variation in the target board pose is required.
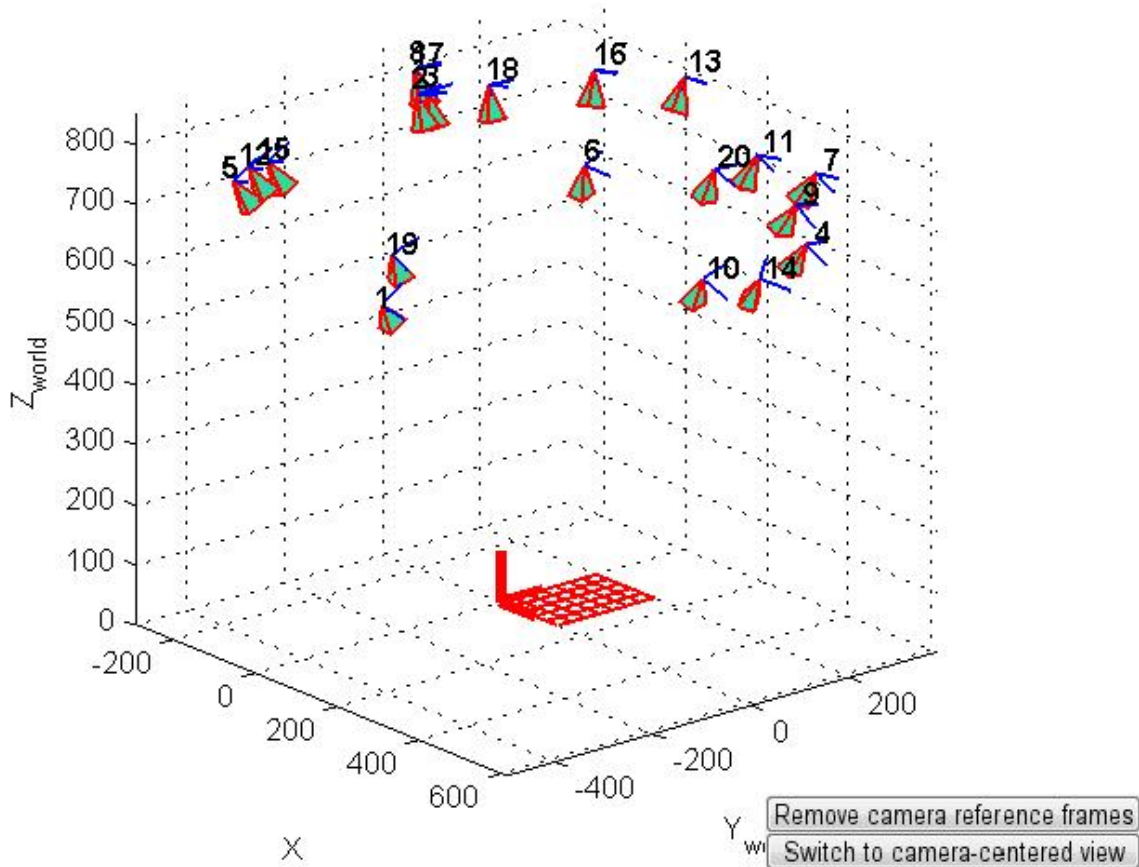
Figure 7: Graphical output of camera orbital view

The orbital view demonstrates how the view point of the camera would have changed when the target board is varied in pose and location (see figures 7). The camera is represented by the pyramids, and the corresponding numbers index each calibration image taken. The orbital view as presented in figure 7 assumes that the target board location and pose remains constant and the camera position and pose vary instead of *vice versa*.

After the graphical output of the orbital view confirmed that the target grids were all the same size, the effective field of view (FOV) was identified, and extrinsic parameters calculated.
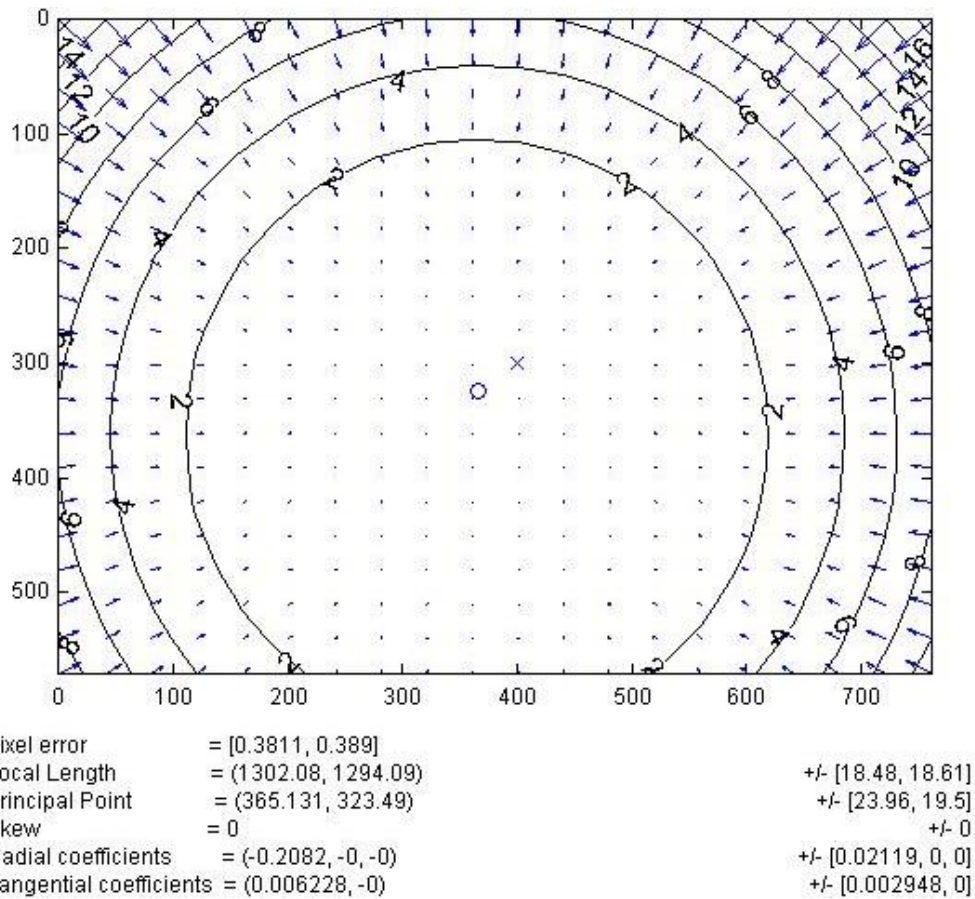
Figure 8: Complete distortion model of extrinsic radial + tangential coefficients

Figure 8 shows the extrinsic parameters that, in this case, were caused by the Pentax ® 6 mm lens. As shown in figure 8, the lens creates a slight distortion that is indicated by the center "O and X" not being coincident.
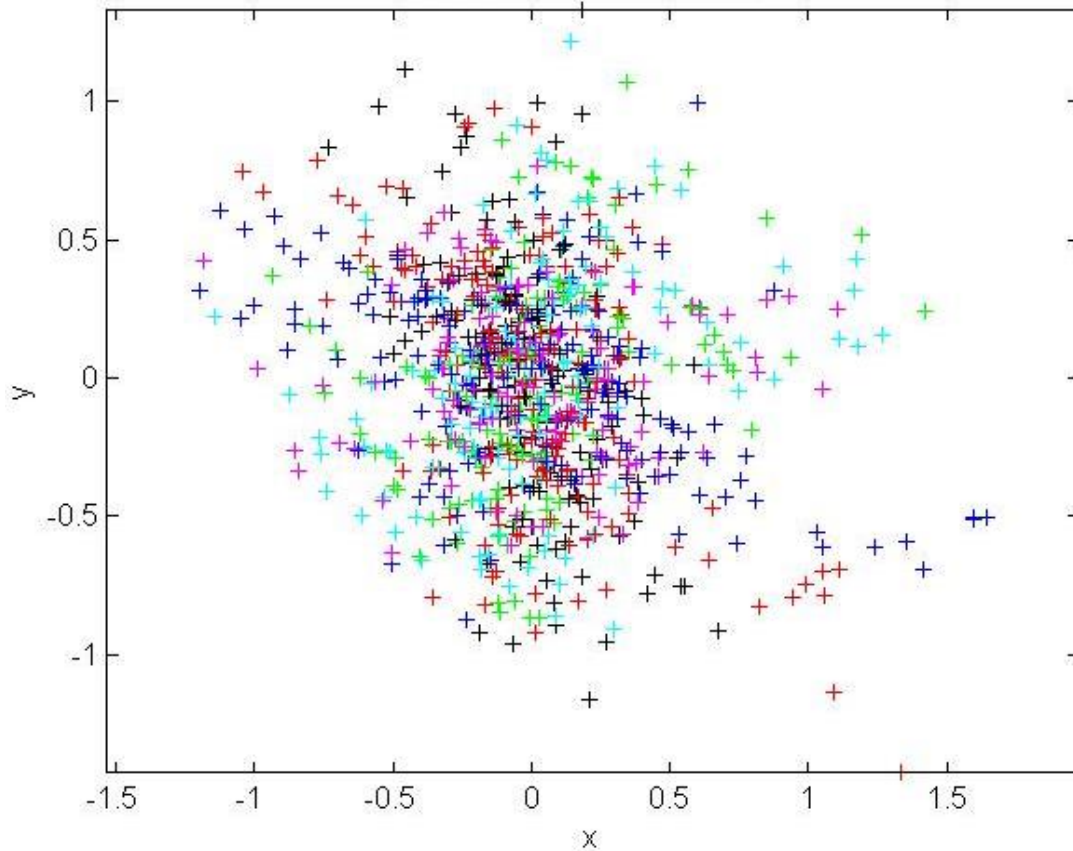
Figure 9: Error report for all 96 selected pixel points. The units of the x and y axes are pixel.

After the extrinsic parameters were calculated, the intrinsic parameters were identified. Multiple colored "+" identified by the pixel error (see figure 9). Once the four common corners were identified during corner extraction, Matlab ® created lattice intersections to mark the other corners of the target board (see figure 6). Each corner represents an origin (0, 0) and the error is established by how far the lattice intersections are from the origin. As shown, most of the error was within the range of 0 to 0.3 pixel. The accuracy with which Matlab ® can determine the width of the ILS in pixels (to determine the stalk diameter) is proportional to this pixel error.

In final step of the calibration process, Matlab ® calculated the intrinsic errors of the camera and extrinsic errors of the lens.

3.2   Corn Cane depth calibration

The distance from the CCD chip of the camera to the target is typically referred to as depth. This variable plays a key role in the measurements of stalk diameters. Depth calibration was accomplished by projecting the laser sheet on a flat surface wile varying the distance from the camera to the laser source from 150 mm to 215 mm. The recorded images are shown in figure 10.
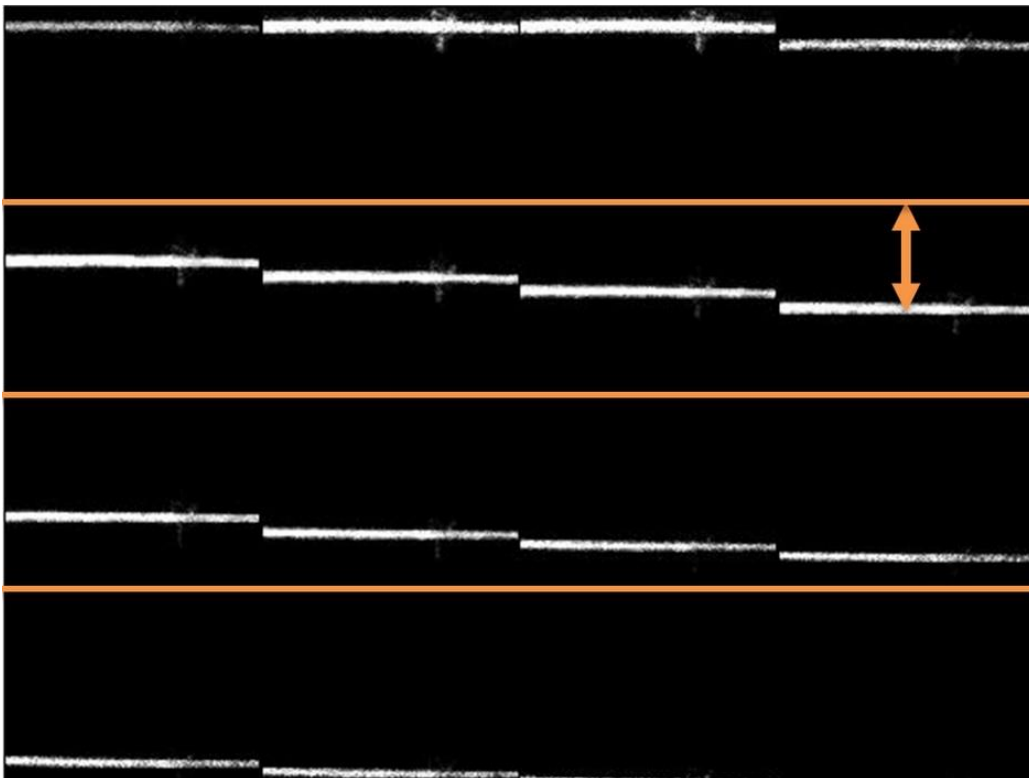
Figure 10: Laser height measurement from images

The depth calibration was conducted by measuring the vertical distance (in pixel), see the vertical arrow in figure 10 from the top of the image to the laser line.
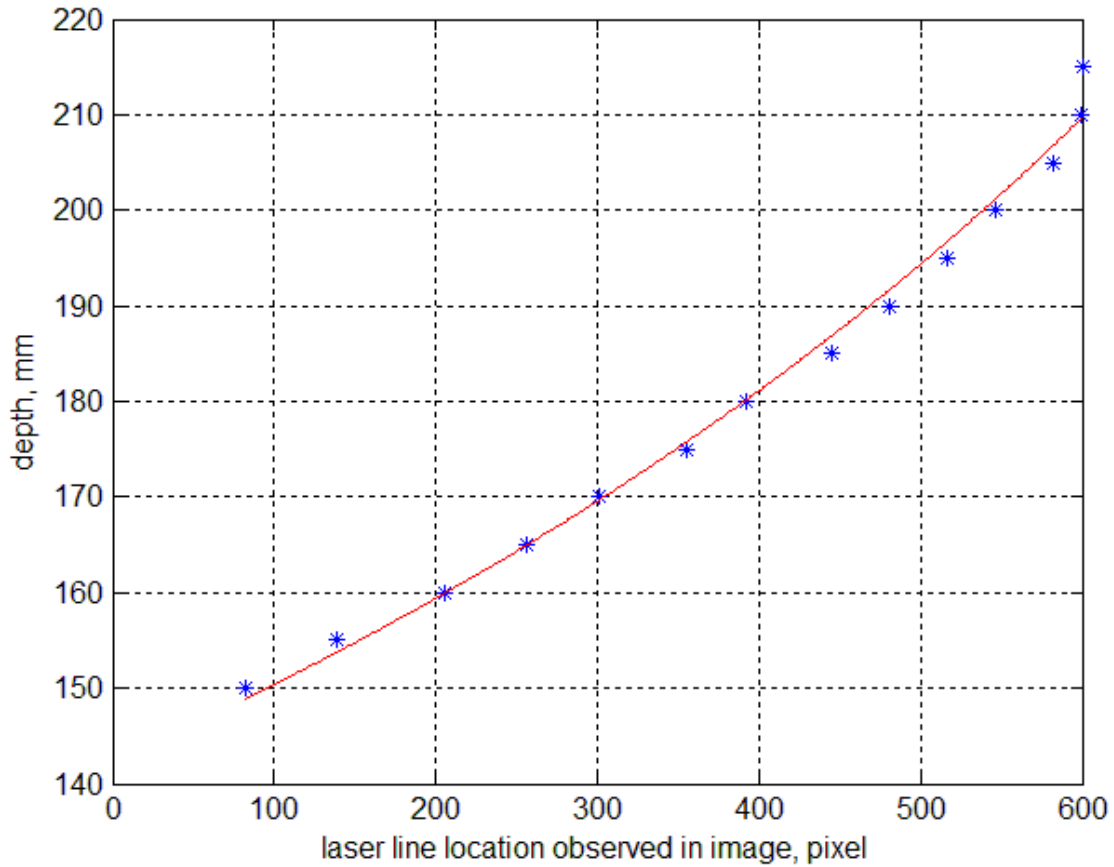
Figure 11: Depth verses laser line location as observed in calibration images

Figure 11 shows the relationship between the depth and the laser line location as observed in the calibration images. The model fitted on data based on the geometer of the camera/laser sheet generator (Zhang & Grift, 2012), yielding a regression coefficient 0.962.

The next step in calibration was to determine a horizontal distance (the width of the ILS) into a stalk diameter. This was accomplished by imaging the target board with known cell widths (28 mm) and relate this to the observed cell with by the camera. Combining this factor with the depths, allows for accurate measurement for any objects dimension using the imaging system.
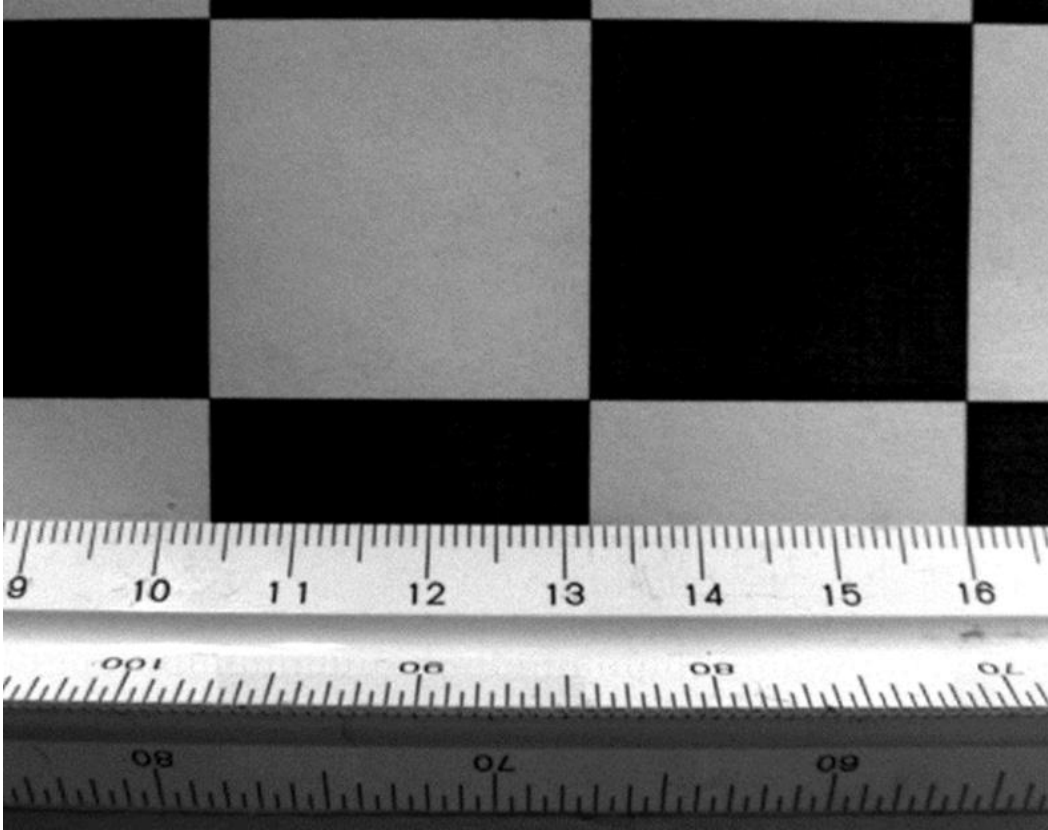
Figure 12: Camera depth calibration by means of image resolution

Figure 12 shows the relationship between the camera resolution in mm per pixel and the measured depth in mm. A linear fit was applied to the data where the depth in mm was obtained from the data as shown figure 13 yielding correlation coefficient 0.992 (Zhang & Grift, 2012).
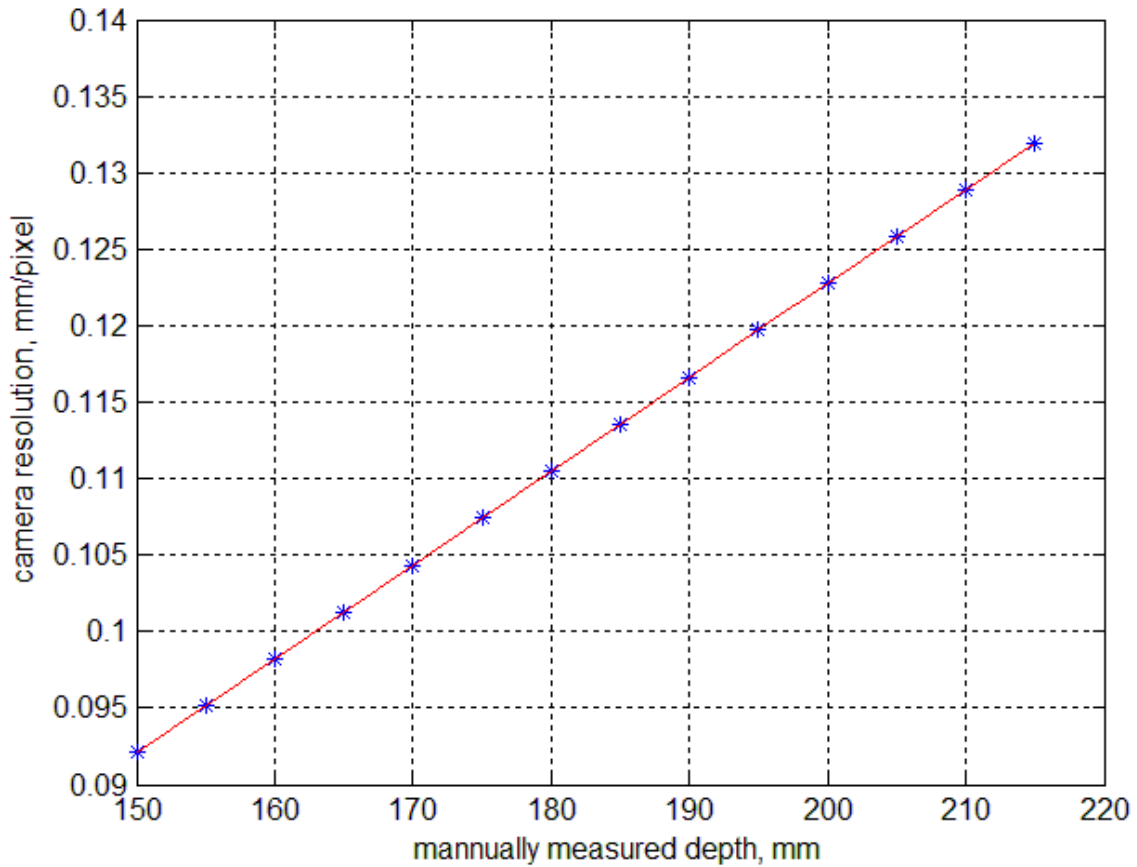
Figure 13: Camera resolution in mm per pixel verses manually measured depths in mm

3.2.1 Corn stalk measurement implementation

The initial corn stalk measurement system was mounted on a three wheeled cart that was 76.2 cm wide to fit between typical corn rows. The cart held a computer for an instant display of the camera images, as well as its own DC power supply. The sensing mechanism was mounted at the bottom right side of the cart and only had the ability to image and analyze one plant at a time (see figure 14).

Figure 14: Imaging system mounted on a cart. Note the slanted laser sheet generator above the camera.

A blade was constructed to deflect interfering objects such as leaves from the view of the camera (see figure 15).

Figure 15: Measurement cart showing the deflection blade and projected laser sheet

During the greenhouse experiments, the cart design was found to be unfeasible since, the wheels of the cart were incapable of traveling through moistened or wet soil, rendering maintain a constant speed difficult. In addition, the wheels caused shaking which negatively affected the imaging process.

Because of these issues, a new platform named the "Corn Cane" was designed and constructed (see figure 16). This method proved more robust than the cart design. Due to the Corn Cane's feasibility, it was used to collect the data as presented in this study. The Corn Cane consists of a 1 meter long pipe with the laser and camera mounted at the bottom. This new design eliminated concerns regarding terrain changes and soil moisture content. A laser sheet was generated by channeling the laser light through a Fresnel lens. This method enabled the camera to accurately segment the ILS in each image. The fixed angle of the laser sheet with

respect to the shaft of the Corn Cane ensured accurate imaging of the corn stalk, without requiring a perfectly vertical attitude of the Corn Cane.

Figure 16: Corn Cane stalk imaging platform

3.2.2 Corn Cane image acquisition
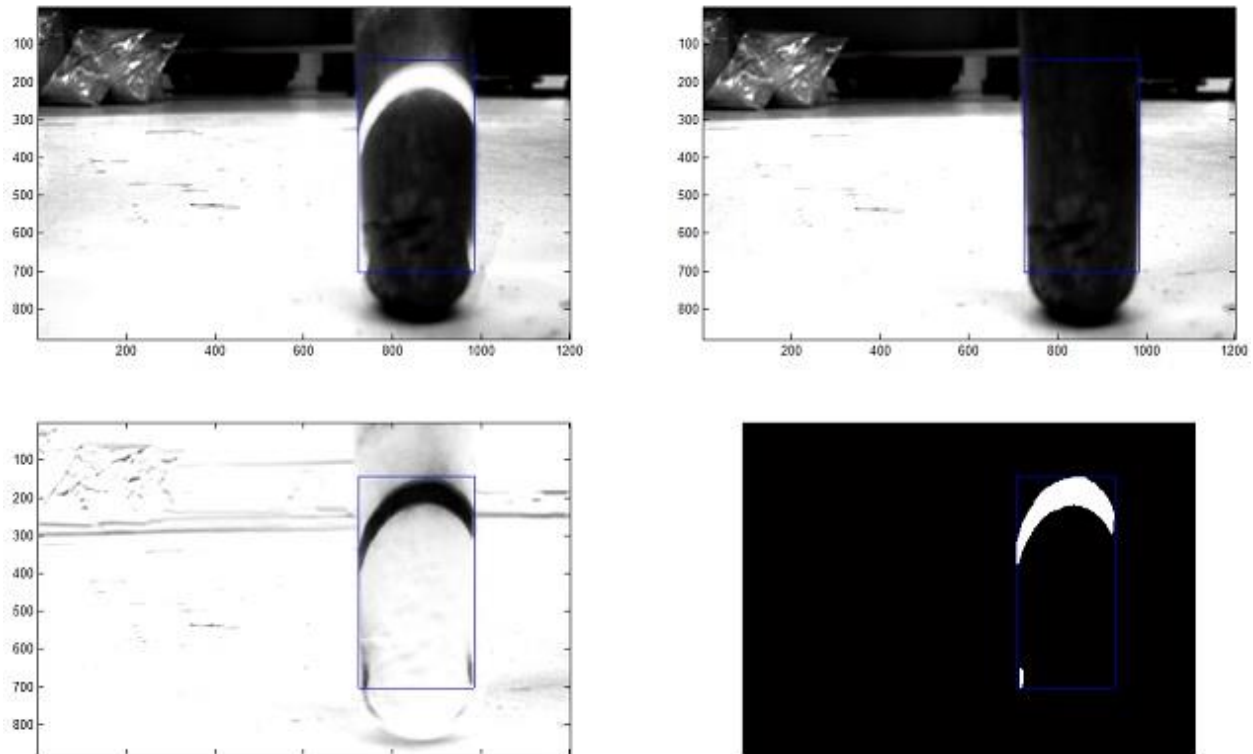
Figure 17: Image subtraction and segmentation in a lab with a PVC tube. Top left: PVC tube with laser crescent. Top right: PVC tube without laser crescent. Bottom left: Difference image. Bottom right: Segmented image creating a prominent laser crescent allowing diameter measurement.

While in laboratory trials, the image subtraction method worked properly (see figure 17), in field tests the method failed due to inevitable motion of the plant. In addition, ambient light made segmentation of the images difficult. The latter problem was solved by adding a bandpass optical filter that matched the wavelength of the laser. This method produced images that prominently showed the laser crescent on the stalks which allowed direct image segmentation, eliminating the need for image subtraction.

To develop a new platform to analyze the diameter of real cornstalks, a laser camera system had to be devised to cope with ambient light and promote clear images even in direct sunlight. Red lasers operated at a wavelength of 635 nm (see figure 18), could not satisfy the demands for optical accuracy in bright sunlight. To compensate for the inability of the camera system to see the red laser, the lens' F-Stop was decreased to allow in more light to the CCD. This reduction in F-Stop size enabled light saturation of the CCD and did not produce images useful for this study.

Figure 18: Diluted YUV image while using the 635 nm wavelength

The limitations of the red laser's brightness in sunlight warranted the adoption of a 50 mW green laser operating at a wavelength of 532 nm. Due to the larger intensity laser sheet on the corn stalk was easier to detect with the Unibrain® Fire-i 701c camera, allowing a reduced

aperture size in the camera, which increases the depth of field. Once the 532 nm laser was selected of the Corn Cane platform, image capturing methods had to be selected. Image subtraction is the method of taking two images in quick succession (see figure 19), and subtracting them. The difference would be the ILS.

Figure 19: Image subtraction approach of the ILS in a real field environment

However, because of wind or a passing clouds, image subtraction was unsuccessful in the task of suppressing all light beside the ILS. Motion of the stalks caused ample imaging noise, rendering inaccurate segmentation of the ILS, and causing inaccurate stalk diameter values.

Figure 20: The difference from figure 19 using image subtraction. Note the background noise

   With image subtraction proving to have errors when eliminating background light from the

ILS in field conditions (see figure 20), new methods were investigated. A bandpass light filter

with a matching wavelength of 532 nm was placed between the Pentax ® 6 mm lens and the

CCD chip of the camera. The brightness intensity of the 532 nm enabled the camera to clearly

distinguish the ILS on the corn stalk, eliminating the need for image subtraction altogether.

Figure 21: The ILS viewed through the 532 nm bandpass filter

The combination of the 532 nm laser and bandpass filter (see figure 21) proved effective especially during corn stalk measurements in edge rows of corn fields that received direct sunlight.

3.2.3   Corn Cane image processing

A 33.1 mm PVC tube was placed on a table top and its physical position to the camera was varied for 100 images. The focus was to ensure that the Corn Cane platform yielded a diameter

result that was accurate and reproducible (see figure 22)
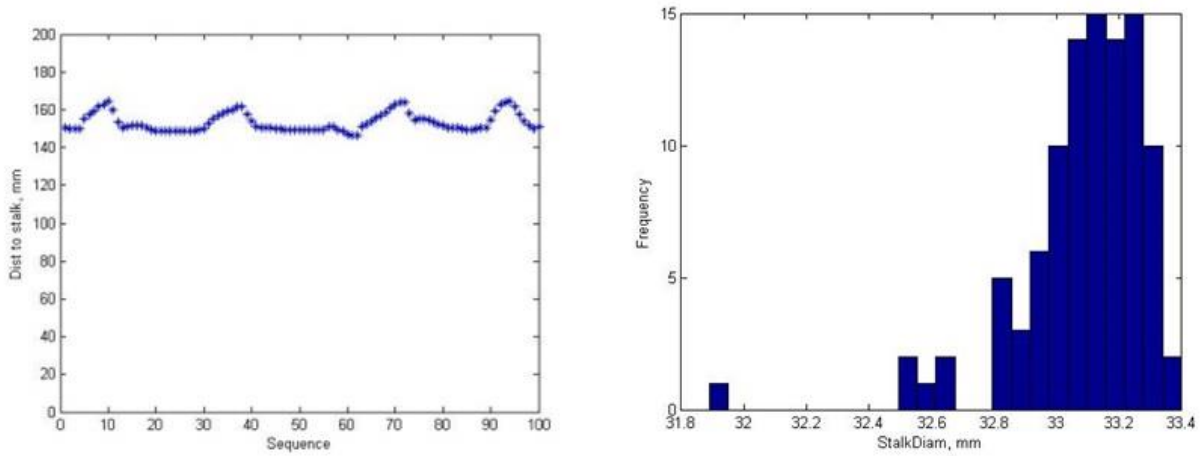
Figure 22: Proof of concept with PVC tubes. Left: Scatter chart indicating the stalks distanced relative to the camera. Right: Histogram indicating the ILS estimates from the Corn Cane. These estimates with a 33.1 mm PVC were 98% accurate.

The images generated with the Corn Cane were segmented into a black and white binary image. A camera trigger threshold of 500 pixels in Matlab® was implemented to identify a fully illuminated corn stalk. This 500 pixel trigger was selected because at that size the F-Stop of the lens did not have to be lowered causing the ILS to appear distorted or to negatively affect the camera's depth of field. Matlab® then recorded the vertical laser pixel height at the highest point, followed by the distance between the widths of the ILS produced by the corn stalk. Once the image was taken and Matlab® also identified the placement of the laser pixels on the image, three equations were used to determine the stalk diameter (Zhang & Grift, 2012). Constants; A, B, and C are representative of the intrinsic parameters of the camera system as found during the calibration process and are given below.

$A = 265,900$
$B = 1,868$
$C = 7.2\ e^{-4}$

$$Distance\ from\ the\ stalk\ (mm) = \frac{A}{(B - Vertical\ Laser\ Height\ (pixel))}$$

$$\frac{mm}{pixel} = C * Distance\ from\ the\ stalk\ (mm)$$

$$Stalk\ Diameter\ (mm) = \frac{mm}{pixel} * Stalk\ Diameter\ (Pixel)$$

The equations used a combination of the intrinsic constants, the manually measured depth, and image resolution to produce the stalk diameter estimate in mm (see figure 23).
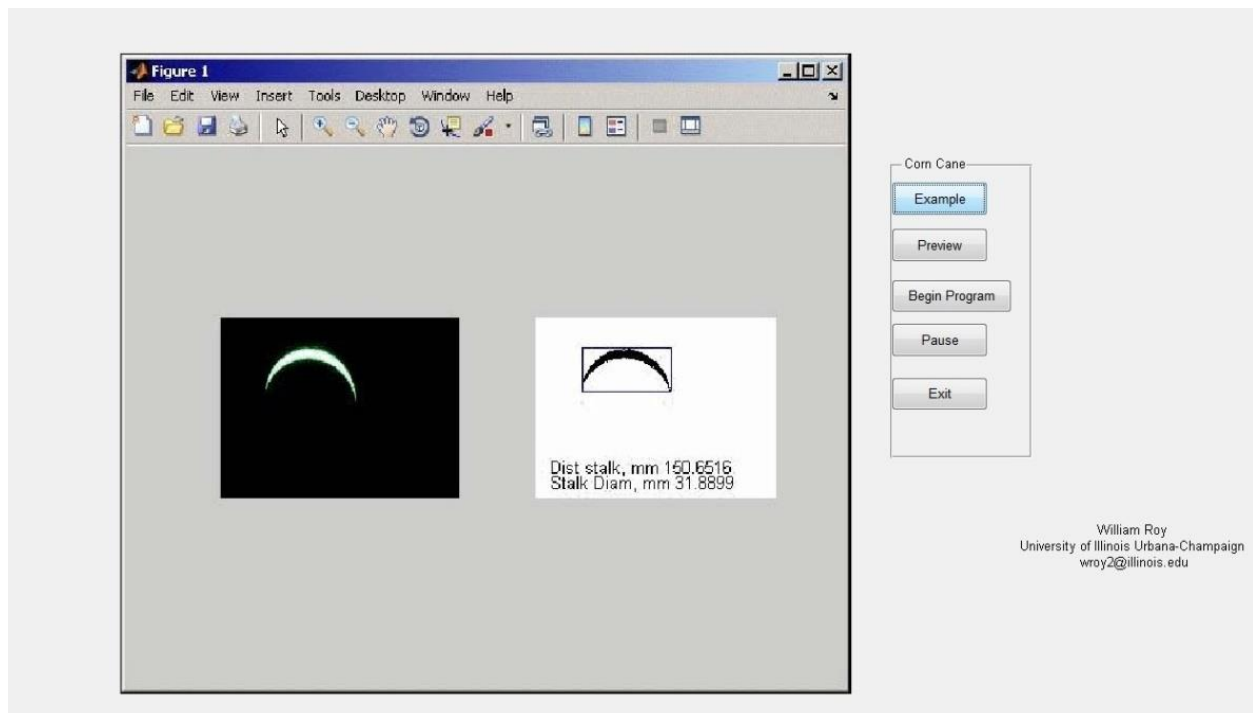
Figure 23: Corn Cane graphical user interface

3.2.4 Corn Cane greenhouse experiments

The stalk diameter measurement performance of the Corn Cane was evaluated in a greenhouse using 126 corn plants. Furthermore, 35 plants were used to establish the correlation between stalk diameters and PPY. To achieve the most realistic field conditions, all environmental parameters were set to emulate central Illinois. The corn variety used was obtained from the University of Illinois Crop Sciences Department and was listed as Dekalb® DKC692-97 (GENVT3P). The greenhouse conditions were monitored and maintained to resemble outside conditions for spring weather of Illinois. A growing period of 120 days was chosen to allow the corn to reach maturity. Ambient heating and lighting had a time schedule starting from 6:00 am to 7:45 pm. The corresponding temperatures ranged from $80° - 85°$ F during the day and $70° - 75°$ F during the night. The windows were unblocked to allow for all sunlight to be present while evaporative cooling was implemented for night-time simulations.

Before the Illinois Drummer soil was used in the green house, it was autoclaved to destroy all pests and disease. After autoclaving, the soil was placed into the greenhouse filling a 60.96 cm deep pit, creating the base floor for planting.

A fertilizer treatment of nitrogen, phosphorous, and potassium (N/P/K) was injected into the soil at a concentration of 300 mg/kg at planting time. Every two weeks for the continuation of the study, pesticide treatments were administered.

Corn seeds were planted at 10.16 cm spacing with 76.2 cm row spacing. All seeds were hand planted at a depth of 8.9 to 10.16 mm. Irrigation lines were installed to the side of each row within 5.08 cm of the planted seed to ensure proper watering methods. All accidental double planted seeds were manually removed either at the time of planting or at the first sign of emergence to avoid overcrowding and stunting.

Figure 24: Corn in the greenhouse study at the germination and emergence (VE) stage

Germination was noted at 6 days after planting (see figure 24). Irrigation was maintained constant along with all lighting and heating conditions to ensure constant growth.

Figure 25: Corn in the greenhouse study at the V3 stage

Twenty days after emergence, all double plantings and weeds were removed. Once this stage was reached, the plants were monitored until true stalks began to develop. At the V3 growth stage (see figure 25), no diameter measurements were taken because the central shoot is not classified as a stalk at this growth stage.

Figure 26: Corn in the greenhouse study at the R1 stage

Eighty-eight days after silking, the crop began to produce ears as well as fill kernels inside of the ears (see figure 26). The laser system was introduced at this stage, and phenotyping was initiated. The first diameter measurements were conducted with electronic calipers. However when the cart was used for the second measurements it proved unable to complete the task: Image variability created by the cart demanded for the Corn Cane to solely be used for image collection

3.3   Below ground phenotyping

The objective of below ground phenotyping was to produce a system capable of collecting high-resolution images of corn stalk root clusters. The instrument for this task is typically termed a Rhizotron, and its purpose is to visualize the development process of plant roots (see figure 27).
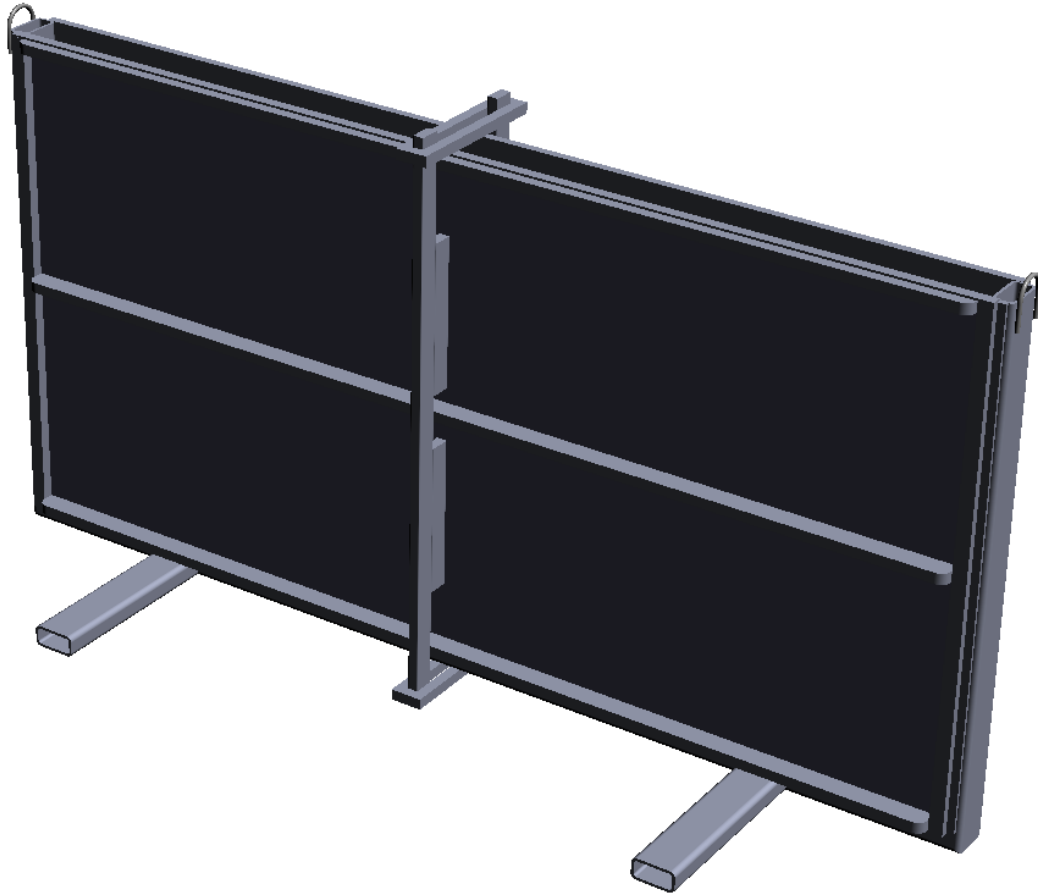
Figure 27: CAD rendering of the growing chamber of the Rhizotron

The Rhizotron research required the following activities:

1.   Construct a physical growing chamber allowing for corn roots to be imaged without reflections during growth.

2.   Construct a frame that holds/positions the machine vision system.

3.   Collect images of root structures free of reflections or obstructions to gain the ability to create inferences about root structure and aggregate parameters.

3.3.1   Rhizotron construction

The concept of a growing chamber was based on the use of a 4.76 mm channel iron to create the frame walls of chamber. The iron frame has the dimensions of 1219 mm by 127 mm by 1219 mm creating a growing area of 0.1887 m^3 (6.66 ft^3) for the corn plant. The front viewing face comprised of a 1168.2 mm by 10 mm by 1168.2 mm thick glass pane, and the back plane was made from water treated plywood.

3.3.2   The Rhizotron Hanger

The second component of the Rhizotron is the Hanger. The concept of the Hanger was based on an iron frame attached to the front face of the Rhizotron. The 90° arms attach to the top support bar of the Rhizotron's growth chamber, while the bottom legs rest on the base of the Rhizotron. While the Hanger is attached to the growth chamber, the linear actuator and black camera cart travel the height of the Rhizotron and image the roots structures.
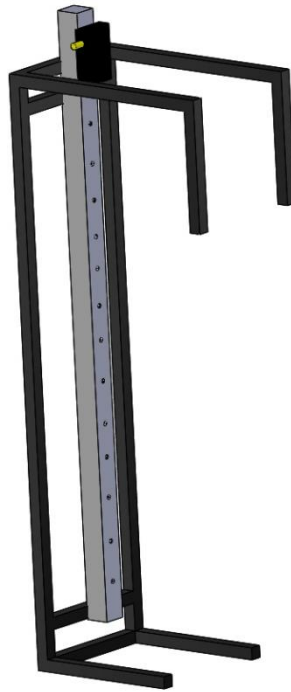
Figure 28: CAD rendering of the Rhizotron Hanger

The Hanger's function was to ensure that the distance between the glass window and camera remained constant (see figure 28). The Hanger was electronically controlled through a USB to Serial connection attached to a Pontech ® STP-101 stepper motor controller board, controlled by MatLab®. A Jameco Replia Pro stepper motor connecting to the linear actuator (Isel, Germany AG ®, Eichenzell Germany), gave the camera the ability to vertically travel the entire length of the chamber. When the camera traveled to the desired location of the corn root structure, the STP-101 through pin #8 of the STP-101 Digital I/O sent a +5 volt signal to a Kyoto ® solid state relay enabling a solenoid to push the camera shutter button of an iPhone4®. Each image was 5 MB in size and the goal was to have the fine details of the root and root structure displayed clearly throughout each image.

Unlike the Unibrain® Fire-i 701c camera used for the Corn Cane, the iphone4® was selected. The iPhone 4® came equipped with a rear mounted 5 mega pixel camera. This camera allowed for a sharper resolution of the corn roots and even the fine root hairs. The 0.48 MB images that the Unibrain® Fire-i 701c produced for the Corn Cane platform would not have been able to produce images of the same quality. The iPhone 4®' proprietary camera software had the ability to focus automatically on the root systems. While using the Unibrain® Fire-i 701c once the parameters were manually adjusted via Matlab®, they remained in that setting until the program ended. Each different set of images would have required a reset of the parameters.

The key issue with attempting to image root structures through a glass pane is reflections. These reflections decrease the images usefulness, and impede the view of the root structures. To restrict the presence of these reflections a black veil was hung from the hanger, in front of the camera, and the camera viewed the Rhizotron through a hole in the veil. To demonstrate the issue of reflections, in the laboratory the idea of image subtraction again was pursued. Here, one image is acquired with and another without the veil in front of the camera. Under the assumption that the reflections were the only changing variable during the imaging process, subtracting the images theoretically results in a difference image in which only the reflections were present. While the veil removed reflections, most light was removed as well. This forced the images to become too dark. In response, an incandescent T-3 lamp was placed on the right side of the Rhizotron between the veil and glass window. This addition provided for illuminated reflection free images, however light washout was noticed on several images.

3.3.3   Rhizotron camera calibration

An iPhone 4® camera calibration was a necessary part of the building procedure. With the use of a checkered target board the image size was determined in both the digital and

physical domain. All Rhizotron images had a vertical height of 2,590 pixels and width of 1,934 pixels, for a total of 5,009,060 termed a five megapixel image.
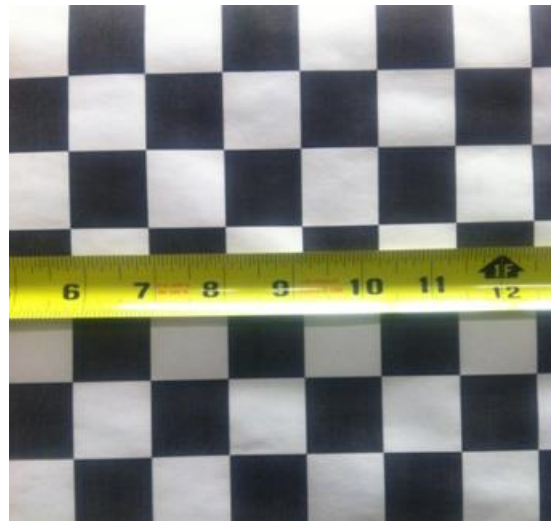
Figure 29: Image resolution calibration for the Rhizotron iphone4®

With a ruler placed on the target board, the image was measured on the x axis to determine the resolution of the Rhizotron images in pixel per millimeter (see figure 29). The spanning distance of the image was measured at 204.8 millimeters yielding an image resolution of 9.44 pixels per millimeter. The image resolution was used to acquire the millimeter height of the same image.

$$\frac{1934 \ pixels}{204.78mm} = 9.44 \ pixel/mm$$

$$2590 \ pixels * \frac{1mm}{9.44pixels} = 274.8 \ mm$$

$$= physical \ image \ size \ of \ 204.78 \ mm \ X \ 274.8 \ mm$$

3.3.4 Rhizotron image reflectance avoidance

Image subtraction was utilized to demonstrate the magnitude of the reflection problem. The ambient light caused these reflections on the entirety of the viewing window obscuring the view of the roots.

Figure 30: Image of the root system without veiled reflection prevention

The first image of the subtraction process was taken in direct light with the iPhone 4® demonstrating the largest problem concerning the presence of reflections. The reflections created an obstructed view of the roots and washed out all details rendering the image unusable (see figure 30).

Figure 31: Image of the root system with veiled reflection prevention

The second (see figure 30) was taken in the same location as figure 31. The veil was raised for this exposure and the iPhone 4® was not hindered by reflections. Figure 31 allows for distinguishing of the root systems much clearer.

Figure 32: Image subtraction differences as shown in RGB (left), binary (right). Left: Subtracted normal image displaying the difference between figures 30 and 31. Right: Subtracted image that displaying the differences as binary between figures 30 from 31 where the white pixels represent the reflections

3.3.5 Rhizotron image processing

Each image had the physical size of 204.78 mm X 274.8 mm. Due to the size of the images to fully view/image the 1,219 mm x 1,219 mm viewing glass from of the Rhizotron, image overlap was imperative. To demonstrate the physical area that each image from the iPhone 4® captured was 56,273.5 mm^2, while the glass face is 1,485,961 mm^2. A grid pattern can be applied to the method of taking images (see figure 33).

1	2	3	4	5	6
7	8	9	10	11	12
13	14	15	16	17	18
19	20	21	22	23	24
25	26	27	28	29	30

Figure 33: Rhizotron window in red with numbered image locations

A total of 30 images will need to be taken to create a digital mosaic of the full face of the Rhizotron. Due to image size, marked in red (see figure 39), images 6, 12, 18, 24, and 30, will have a 5% overlap with the images to their left. When the overlap is completed, Matlab® can use a standard *Stitch* function to create a digital mosaic of the viewing window.

After the RGB image was taken from the iPhone 4®, it undergoes a range of Matlab® functions before it becomes the final image. First the function of *Intensity Adjust* that rescales the color map in Matlab® was applied. This application was set to darken the overall image. Second the darkened RGB image is separated into the blue phase. This blue phase was chosen because it gave the clearest contrast between the background (aggregate) and foreground (root structure). In the final stage, the darkened blue phase image is segmented into a binary black and white image with the threshold function of *Connectivity 8. Connectivity 8* is a function that eliminates all white components (pixels) that are not part of a grouping of 8 or more. An example of the *connectivity* function is given below:

$$
\begin{matrix} 1 & 0 & 0 \\ 0 & 1 & 1 \\ 1 & 0 & 0 \end{matrix} \; (4\;white\;pixels) \; \rightarrow \; Connectivity \; \rightarrow \; \begin{matrix} 0 & 0 & 0 \\ 0 & 0 & 0 \\ 0 & 0 & 0 \end{matrix} = (8\;black\;pixels)
$$

The final outcome of this process was a binary image that only displayed a white corn root body on a solid black background.

3.3.6 Rhizotron soil preparation

A layered approach of pasteurized Illinios Drummer soil and Turface Athletics ® clay was used to fill the growing space of the Rhizotron. 0.4 m³ (1.5 ft³) of Trueface Athletics ® clay was used to fill the bottom of the Rhizotron. 0.14m³ (5 ft³) of pasteurized Illinois Drummer soil was used to fill the rest of the Rhizotron. The layers were to promote proper water flow and drainage so as to not create mold or drown the roots. A corn root uptakes 40% of its water in the first 30.48 cm of soil, while 30% of water uptake is done in the second 30.48 cm (Anderson, 2007). Thus soil along 75% of the chamber height was necessary to the plant. No fertilizer was added to the soil inside of the Rhizotron because the fertilizer had the potential to cloud the view through the glass face (see figure 34).

Figure 34: Front view through the Rhizotron's viewing 10 mm glass face displaying the layers between the Drummer soil and clay located in the bottom

During all growing days until the roots were able to be imaged, the glass pane remained uncovered (see figure 34). Sunlight and artificial lighting from the greenhouse was able to shine into the Rhizotron growth chamber. This caused the growth and development of algae inside of the growth chamber. Green algae grew directly between the glass and roots, which was an unintended outcome.

3.3.7 Rhizotron corn planting

The chosen seed were Dekalb® DKC692-97 (GENVT3P). These seeds were planted ≈ 30.48 mm on center at a soil depth of 7.62 mm. Four seeds were planted in the Rhizotron to give adequate room for each root system to reach full potential.

3.3.8 Rhizotron environmental conditions

Day light growing hours were set from 6:00 am to 7:45pm seven days a week for the duration of the study. Temperatures were set from $80° - 85°$ F during daytime and $70° - 75°$ F during the night with the use of evaporative cooling.

4   RESULTS

4.1   Corn Cane performance evaluation using PVC tubes

The Corn Cane was evaluated using objects with a constant diameter. The objects were PVC tubes that were placed in front of the camera system within the zone illuminated by the laser sheet. The accuracy of the laser sheet remained above 98% for all 100 image tests independent of PVC tube location with respect to the camera (see figure 35).
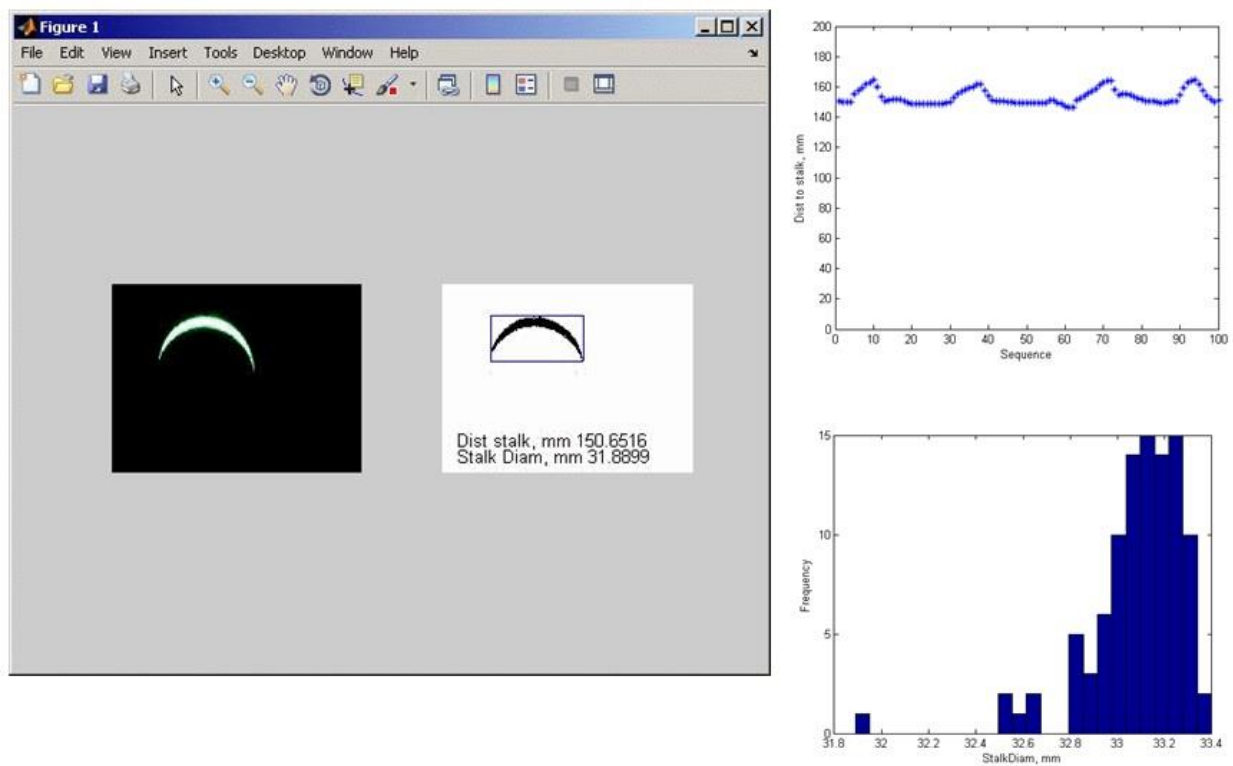
Figure 35: Corn Cane performance evaluation of 33.5 mm PVC tubes. Left: GUI display of the current PVC tube image. Upper right: Measured distance from the camera, acquired by the downward height of the ILS. Bottom right: Histogram of the 100 measurements and their relation to correct diameter of 33.1

Secondary tests were conducted with a smaller PVC tube, with a fixed diameter of 26.7, which demonstrated that the Core Cane has the capacity to image and differentiate the diameters of multiple sized objects (see figure 36).
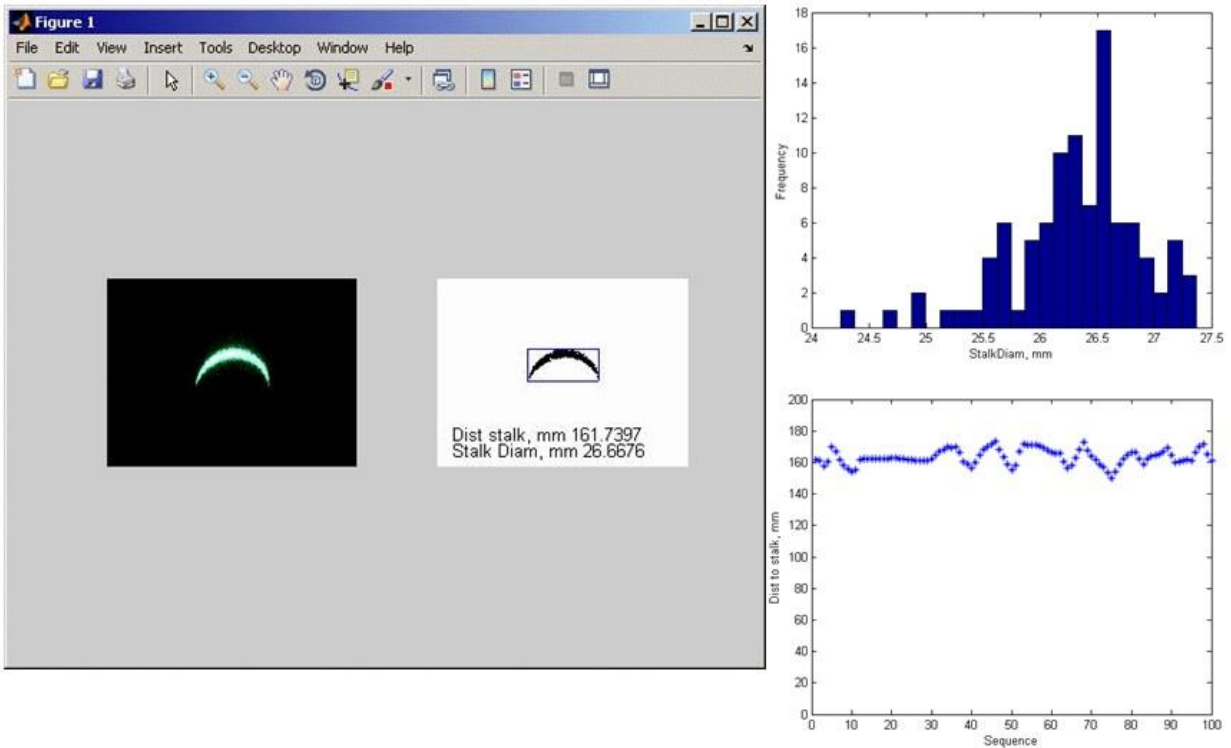
Figure 36: Corn Cane performance evaluation of 26.7 mm PVC tubes. Left: GUI display of the current PVC tube image. Upper right: Measured distance from the camera, acquired by the downward height of the ILS. Bottom right: Histogram of the 100 measurements and their relation to correct diameter of 26.7

With confirmed accuracy of the camera through the calibration process, the Corn Cane was used to expand the application to a greenhouse.

4.2   Corn Cane field evaluation in the greenhouse.

The diameters of 126 stalks were measured using the Corn Cane in a greenhouse study. For comparison these diameters were also measured manually using Pittsburg ® electronic calipers.

It was noted that due to the added variability of oval shaped corn stalks, and non-precise measurement locations, the accuracy of the Corn Cane decreased and yielded a regression coefficient 0.838 (see figure 37).
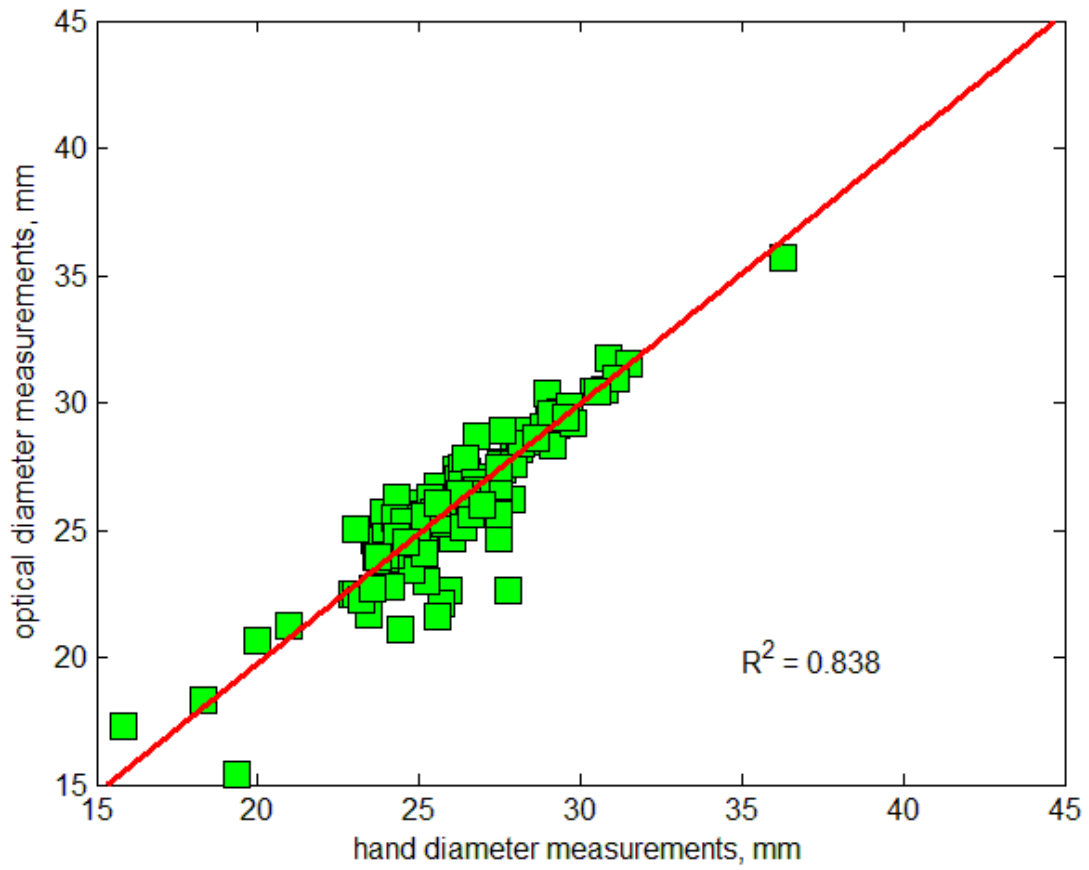
Figure 37: Relationship between caliper measurement and Corn Cane measurements
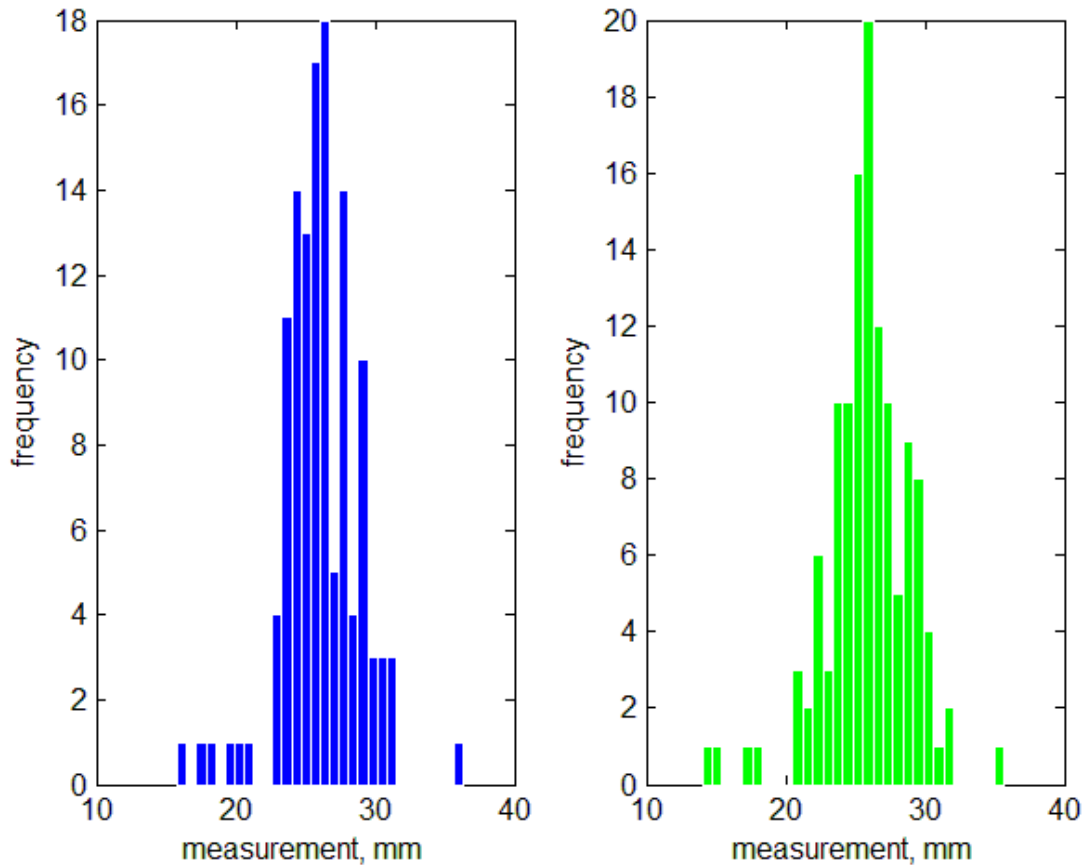
Figure 38: Histograms of both 126 caliper and Corn Cane measurements displaying similar histograms

The histograms of the manual and Corn Cane measurements are similar, and outliers created by field variability can be recognized (see figure 38). In the case of handheld calipers, the average measurement was 26.04 mm with a standard deviation of 2.73 mm. The ILS performed in a similar way with an average measurement of 25.88 mm, standard deviation of 3.05 mm

During performance evaluation, several problems were encountered. A corn stalk does not possess a truly circular stalk at any point in its development. In contrast, as the plant grows, stalks begin to form and the plant will maintain an oval-like shape for the entire life cycle. When comparison measurements were taken with the hand calipers, exact placement on the corn stalk

was enforced, and the laser sheet was positioned at the exact same place of the stalk to ensure as similar measurements as possible.

Low-hanging crop leaves posed a challenge for the Corn Cane, as well for the moving platform cart as shown in figures 8 and 9. When the corn plant entered a mature stage, the V1 and V2 leaves hung down and obscured the corn stalk from the vision of the camera. This lead to false images of corn leaves or partial images of stalks combined with leaves (see figures 39 and 40).

Figure 39: An unusable image, which displayed 3 ILSs

The current Matlab® script used to image and analyze the ILS on the stalk was unable to mend this problem. Due to this error the process is unable to accurately measure the diameter through the ILS, since the sum of the three ILSs will be displayed as the incorrect diameter.

Figure 40: A second incorrect image indicating the horizontal laser length to be inaccurate because of leaf coverage on the stalk adding to the ILS diameter on the left side of the stalk

This issue was resolved with by changing the sampling methods of the Corn Cane. The most common method was if one side of the corn stalk was obscured from view, the collected image would be taken from the stalks other side, assuming leaves did not cover the entirety of the lower 30.48 cm. Another limiting problem arose during the greenhouse study, where five edge row plants developed two ears each (see figure 41).

Figure 41: Double ear crops

The edge row corn plant that inadvertently grew two ears per plant, were removed from the sample population of the Corn Cane study.

4.3   Statistical analysis of physical corn plant properties to yield

Yields are established when the dry weight of grain is taken with respect to area harvested. However, with phenotyping the corn plants an approximate notion of yield can be estimated in reference to the diameter of the corn stalk.

4.3.1   Analysis of diameter to unshelled ear weight.
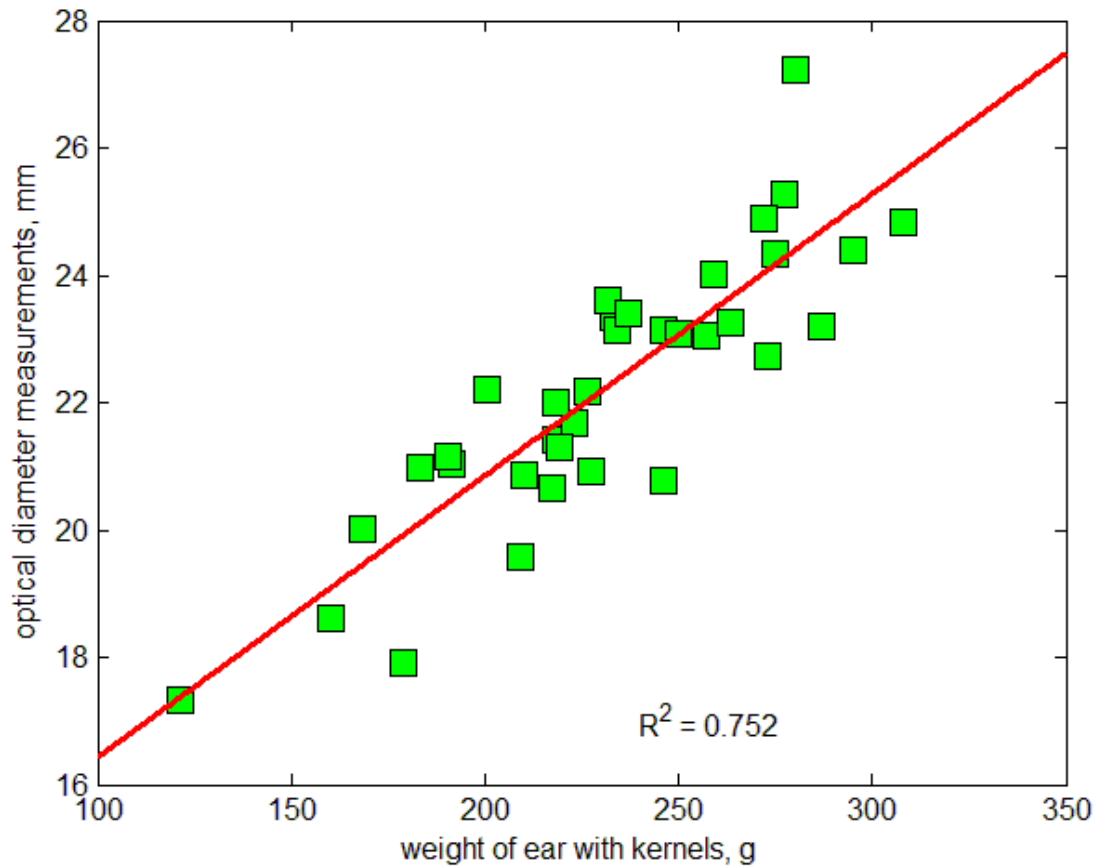
Figure 42: Regression between the Corn Cane measured diameter of the stalk and the weight of the unshelled ear

The linear regression between the diameter of the stalk and the weight of the unshelled corn ear is evidence that larger corn plants create larger crop ears. The analysis of the corn stalks and ear weights yielded a strong linear regression coefficient 0.752 (see figure 42).

The 35 corn plants yielded a total ear weight volume of 8,089 grams, an average of 231.12 grams and a standard deviation of 41.29 grams. All collected weights included the physical corn cob.

4.3.2 Statistical analysis of diameter to kernel weight

Commercially all yields are recorded by mass per area. Yields do not include the actual cob weight, thus questioning the relationship between total kernel weight and the stalk diameter.
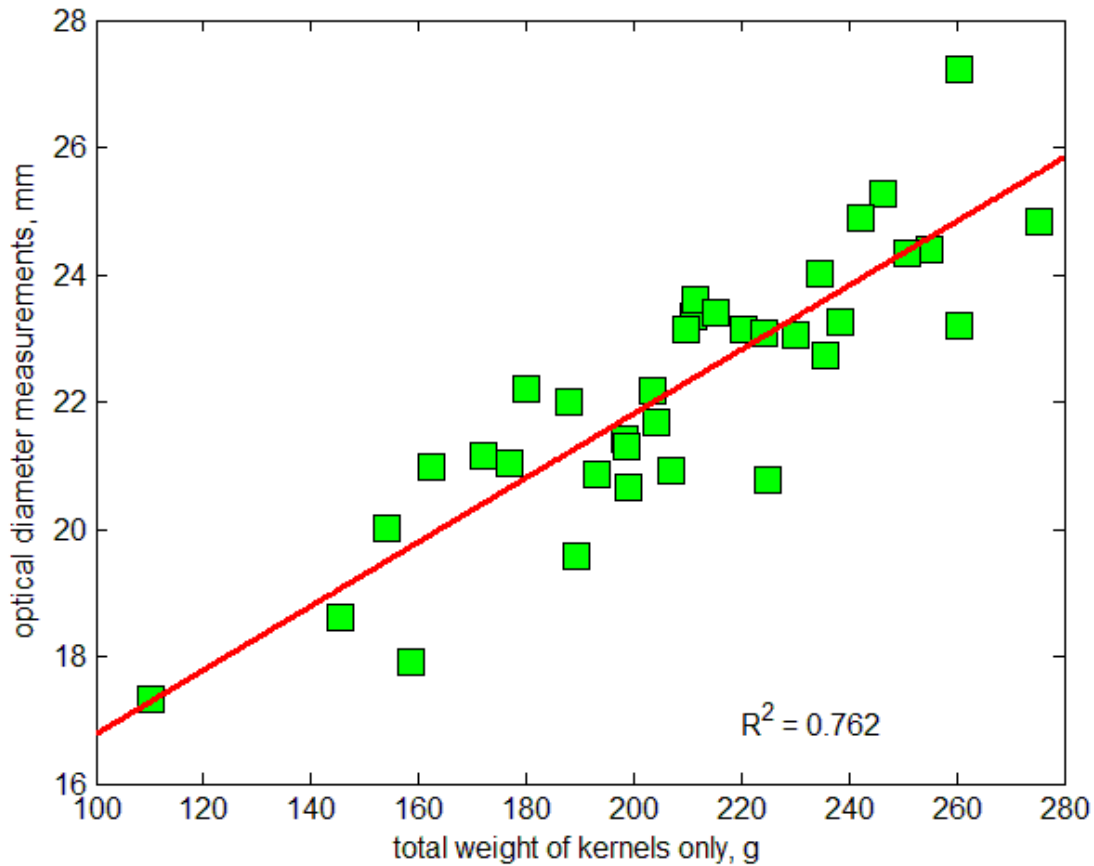
Figure 43: Regression between the diameter of the stalk and the kernel weight

Once the kernels were removed from cobs, the regression between individual plant yield to individual stalk diameter improved by 0.01(see figure 43). It was determined that the total

yield of the kernels for the 35 plants was 7,286 grams. The average weight per corn plant was 208.19 grams with a standard deviation of 36.61grams. There was a strong regression coefficient of 0.76 between the Corn Cane diameter measurement and total weight of the kernels per corn ear (see figure 47).

4.3.3   Rhizotron results

The Rhizotron created a platform enabling the study of the root systems of a corn plant. With the absence of reflections from the glass viewing window, all images without algae displayed the root systems in fine detail.

4.3.4   Rhizotron environmental obstacles

Few images suffered from an algae infestation, and "light washout" from imbalanced lighting created by the incandescent T-3 lamp. With both cases these ailments rendering the images unusable due to the camera's view of the roots became obstructed (see figure 48).

Figure 44: Unusable Rhizotron image due to algae blocking the view of the roots. Note light washout on the right of the image

Algae had grown inside of the growth chamber during the roots' growth time. This was caused by allowing the front viewing window to light during the entirety of the growing period. As a result of the algae, many quadrants of the Rhizotron's glass face unable to display the roots adequately for image collection (see figure 44).

4.3.5   Rhizotron soil characterization

As stated, a useful image was created when the root systems were visible to the camera, the absence of algae, and absence of reflections (see figure 45).

Figure 45: Successful Rhizotron image before Matlab® rendering

Having the ability to image the corn roots within the soil of Rhizotron created a new platform from which inferences could be formed. A preliminary results based on the collected images of the Rhizotron, was that root growth is affected by soil aggregate size.

4.3.6   Rhizotron root size estimation

Once the image was collected and separated into its blue phase, it was segmented into a binary image. This created the best contrast to view larger nodal roots (see figure 50). With the knowledge of the resolution and the clarity of the image, root length estimations were made. The

estimations were just examples of what the root length could have been due to corn roots are not continuous, nor develop fully exposed to the glass. For instance, the nodal root in figure 46 was estimated to be 74.48 mm long. The deeper these nodal and seminal roots travel into the soil the better the corn plant can prevent lodging and promote growth.
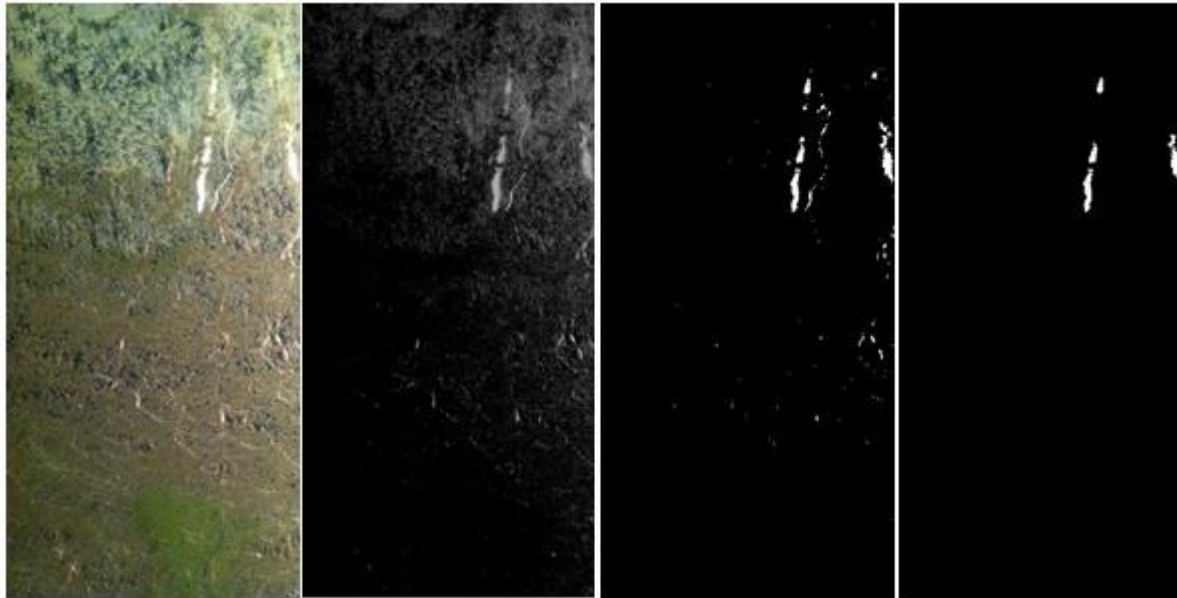
Figure 46: Complete nodal root image with successful Matlab® rendering. Left: Original Rhizotron image collected from the digital camera. Inner left: Red and Green phases were removed from the image. Inner Right: Intensity Adjustment was reduced -75%. Right: White Pixels in groups smaller than 7 were segmented away, only to leave the nodal root in the image

4.3.7 Rhizotron root behavior in different aggregate types

Currently the Rhizotron platform does not have the ability to quantitatively measure the aggregate size or the spacing between particles. It does however have the ability to visually assess root behavior in different aggregate size areas. With the layered combination of Drummer soil and Trueface ® clay roots were forced to make "growing decisions." While the entire root may not be seen, the decisions made are visible through the glass with the use of the images that

the Rhizotron created. Figure 47 shows how a root system traveled and estimated 914 mm

downward through the soil following the drainage path of water until it reached the clay
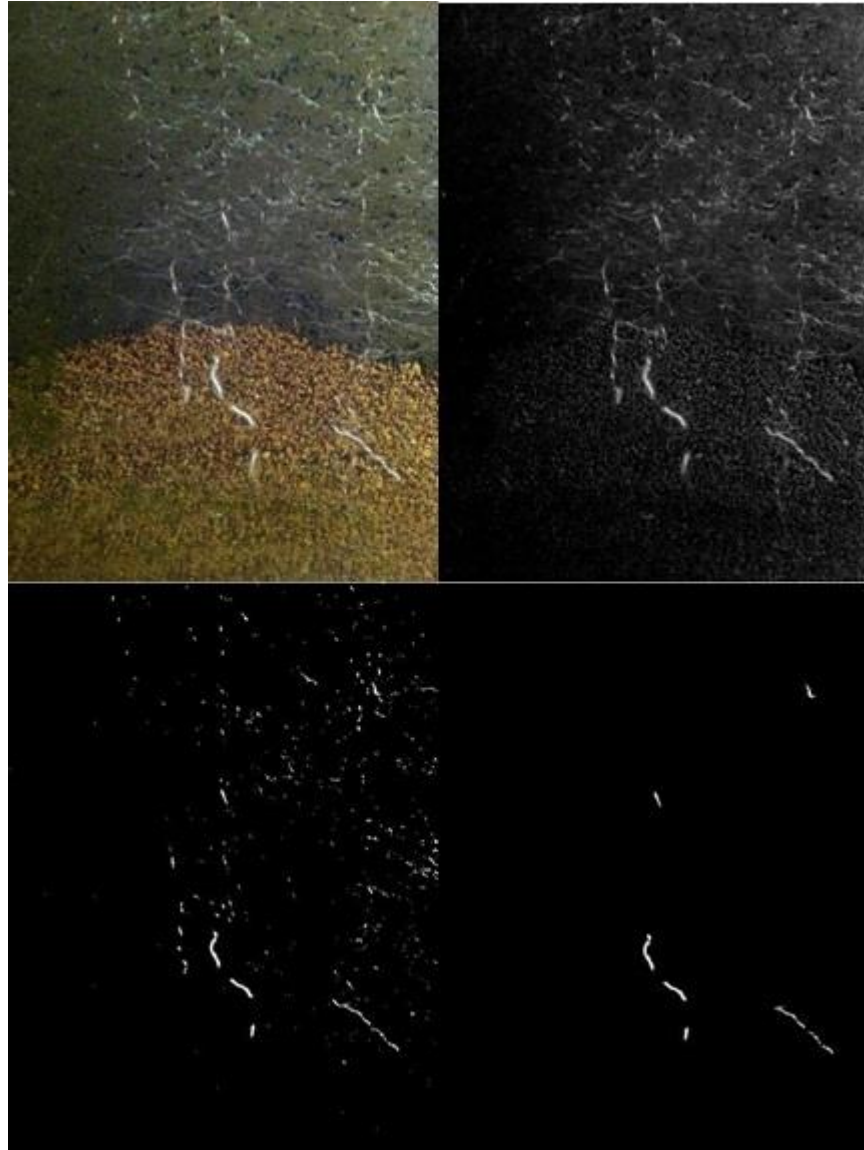
Figure 47: A second complete seminal root image in different aggregates with Matlab®
rendering. Upper Left: Original Rhizotron image collected from the digital camera. Upper Right:
Red and Green were removed from the image. Lower Left: Light intensity was reduce75%.
Lower Right: White Pixels in groups of 7 or less were segmented away, only to leave the seminal
root in the image.

5   CONCLUSIONS/RECOMMENDATIONS FOR FUTURE STUDY

The Corn Cane demonstrated to have a useful application in plant phenotyping, with a portable platform to image the corn stalks' diameter and a stationary platform to image root structures at a high resolution.

During the Corn Cane study, a greenhouse experiment was conducted to emulate field environments to eliminate lab bias due to the noticed variability between PVC tubes and real corn plants. Image segmentation proved to be a useful and powerful tool to clearly display strong foregrounds and backgrounds within each image for both phenotyping platforms. With that the ability to accurately phenotype the corn stalk a strong linear correlation 0.762 between diameter and yield, indicated the correlations between phenotyping the diameter of the corn stalk to the individual grain yield of a plant (see figure 52).

The Corn Cane is a new measurement platform that had been created allowing for a quicker method of measurement, on the grounds of the correlations of the physical parameters of the crop for an estimation of yield. The Corn Cane's real-time applications and ease of use make this platform a robust tool to phenotype corn stalks.

Much can be done to improve upon the Corn Cane platform. A list of recommendations is given below.

1.   A larger outdoor study should be conducted to strengthen the current study's claim of stalk phenotyping and its correlation to PPY.

2.   Laser sheet alternatives should be studied, with the utilization of other filters. There could be a wavelength that appears much clearer on the corn stalk and can deal with the issue of low hanging leaves (see figure 44).

3. A laptop was carried through the corn during this study. For safety and security a form of wireless data transferring should be implemented. All studies were halted upon the laptop dying and needing charging. Also a network storage drive or cloud should be implemented to give the operator more space for images in a large scale experiment.

4. Matlab ® scripts should be created to compensate for multiple ILSs within images.

The Rhizotron platform demonstrated to be useful in producing clear, high resolution images of corn roots in different aggregates of the growth chamber. The images were captured with the aid of the Hanger/camera system and were reflection-free, with the use of a black felt veil hung from the framework.

Figure 48: High resolution Rhizotron image of the root system in Drummer soil and Trueface ® clay

These images have the potential to aid in phenotyping by means of analyzing the root structures below the soil (see figure 48). At this stage, no numerical data can be claimed but inferences about the behavior of root systems, or root structure physical size can be made.

Much can be done to improve upon the Rhizotron platform. A list of recommendations is given below.

1.   Another growth chamber should be prepared and imaged without the presence of algae.

2.   A correlation between kernel weights to root complexity should be determined. If a relationship can be found then different hybrids can be chosen for different soil types thus maximizing yields.

3.   A multi-hybrid seed study for the Rhizotron would be useful. A correlation between root depths to growing time could give insight to how different nodal roots become brace roots quicker, creating a stronger plant faster.

4.   Ambient lighting should be controlled to create a more uniform image in terms of light wash out before segmentation.

5.   The Rhizotron growth chamber should be painted black to eliminate reflections from the yellow body rails.

6.   Controlled lighting should be established for imaging the root structures. The unbalanced lighting currently creates a large amount of segmentation issues.

5.1   Applications of the study

The Corn Cane platform constitutes an innovative way to measure the diameter of the corn stalks. Through a greenhouse study, a relationship was established between the diameter of the corn stalk and PPY. However PPY can be impacted by a variety of factors and parameters within the corn plant or its surroundings, whereas the Corn Cane focused on merely one parameter. Although the data showed a positive correlation between corn stalk diameter and PPY, the range of diameters was too limited to show if and where the PPY increase would level off.

The Rhizotron platform was created as a tool to image root structures visible behind a glass pane. The automation technology in the platform allows for rapid acquisition of high-resolution imagery that can be used to study the development of the root system in relation to growth parameters: The semi-automated Rhizotron can potentially fill a key role in hybrid corn development within both academia and industry. Once the image processing techniques are mature, commercial seed companies would have a tool to study root architecture development *in-*

situ. Depending on the size of the Rhizotron, soil types could be paired with hybrid corn seeds to determine which genetic traits of the corn best match its growing environment. This may contribute to the acceleration of corn yield increases worldwide, which is a key requirement to keep pace with a growing global population.

6   REFERENCES

Anderson, L. (2007, December 7). *North Dakota State University* . Retrieved May 30, 2013, from http://puc.sd.gov/commission/dockets/hydrocarbonpipeline/2007/Hp07-001/hearingexhibit/anderson/landerson13f.pdf

Bouguet, & Jean-Yves. (2010, July 9). *Camera calibration toolbox for matlab*. Retrieved March 5, 2012, from http://www.vision.caltech.edu/bouguetj/calib_doc/

Cahn, M. D., Zobel, R. W., & Bouldin, D. R. (1989). Relationship between root elongation rate and diameter and duration of growth of lateral roots of maize. *Plant and Soil* , 2:271-279.

Calfee, L. R. (2003). *Post-transplant of landscape-sized shade trees.* Blacksburg, VA: Virginia Polytechnic Institute and State University.

de Dorlodot, S., Forster, B., Pages, L., Price, A., Tuberosa, R., & Draye, X. (2007). Root system architecture: opportunities and contraints for genetic improvement of crops. *Science Direct*, 12:474-481.

Dignat, G., Welcker, C., M, S., Ribaut, J. M., & Tardieu, F. (2012). The growths of leaves, shoots, roots, and reporductive organs partly share genetic control in maize plants. *Plant Cell and Environment*, 58:425-435.

Duvick, D. (2005). The contribution of breeding to yield advances in maize (zea mays l.). *Advanced Agronomics*, 86:83-145.

Eberius, M., & Lima-Guerra, J. (2009). High-throughput plant phenotyping data acquisition, transformation, and analysis. In D. Edwards, *Bioinformatics: Tools and Applications* (pp. 259-278). Springer Science+Business Media, LLC.

El-Lithy, M. E., Reymond, M., Stich, B., Koornneef, M., & Vreugdenhil, D. (2010). Relation among plant growth, carbohydrates and flowering time in the arabidopsis landscape erecta x kondara recombinant inbred line population. *Plant Cell and Environment*, 33:1369-1382.

Garrigues, E., Doussan, C., & Pierret, A. (2006). Water uptake by plant roots: I-formation and propagation of a water extraction front in mature root systems as evidenced by 2D light transmission imaging. *Plant Soil*, 283:83-98.

Goodman, A. M., & Ennos, A. R. (1999). The effects of soil bulk density on the morphology and anchorage mechanics of the root systems of sunflour and maize. *Annual Botany*, 83:293-302.

Grift, T. E., Bohn, M., & Novais, J. (2011). High-throughput phenotyping technology for maize roots. *Biosystems Engineering*, 110:40-48.

Hackett, C., & Rose, D. A. (1972). A model of the extension and branching of a seminal root of barley, and its use in studying relations between root dimensions. *Australian Journal of Biology*, 25:669-679.

Hammer, G. L., Kropff, M. J., & Porter, J. R. (2002). Future contributions of crop modeling - from heuristics and supporting decision making to understanding genetic regulations and aiding crop improvement. *European Journal of Agronomy*, 18(2):15-31.

Huck, M. G., & Taylor, H. M. (1982). The rhizotron as a tool for root research. In *Advances in Agronomy* (pp. 35:1-33). New York, New York: Academinc Press Inc.

Kooistra, M. J., Schoonderbeek, D., Boone, F. R., Veen, B. W., & van Noordwijk, M. (1992). Root-soil contact of maize, as measured by a thin-section technique. *Plant and Soil*, 139:119-129.

Kuchenbuch, R. O., & Ingram, K. (2004). Effects of soil bulk density on seminal and lateral roots of young maize plants. *Plant Nutrition* , 167:229-235.

Lobet, G., & Draye, X. (2013). Novel scanning procedure enabling the vectorization of entire rhizotron-grown root systems. *Plant Methods*, 9:4-10.

McDougall, W. B. (1916). The growth of forest tree roots. *American Journal of Botany*, 3:384-392.

Mooney, S. J., Pridmore, P. T., Helliwell, J., & Bennentt, M. J. (2011). Developing x-ray computing tomography to non-invasively image 3D root systems archetectures in soil. *Plant and Soil*, 352:1-22.

Munns, R., James, R. A., Sirault, X. R., Furbank, T., & Jones, G. H. (2010). New phenotyping methods for screening wheat and barley for beneficial responses to water deficit. *Journal of Experimental Botany*, 61:3499-3507.

Parant, B., & Tardieu, F. (2012). Temperature responses of developement processes have not been affected by breeding in different ecological areas for 17 crop species. *New Phytologist*, 194:760-774.

Payero, J. O., Tarkalson, D. D., Irmak, S., Davison, D., & and Petersen, L. J. (2009). Effect of timing of a deficit-irrigation allocation on corn evapotranspiration, yield, water use effiency and dry mass. *Agricultural Water Managment*, 96:1387-1397.

Tang, A. C., & Boyer, J. S. (2002). Growth-induced water potentials and the growth of maize leaves. *Journal of Experimental Botany*, 53:489-503.

Ugoji, E. O., & Laing, M. (2008). Rhizotron studies on zea mays l, to evaluate biocontrol activities of bacillus subtilis. *World Journal of Macrobiol Biotechnology*, 24:269-274.

University of Nebraska at Lincoln . (n.d.). Retrieved April 9, 2013, from Plant and Soil sciences elibrary: http://passel.unl.edu/pages/informationmodule.php.

Wiley, R. W., & Heath, B. S. (1969). The quantitative relationship between plant population and crop yield. *Advances in Agronomy*, 21: 281-321.

Wolkowski, R. P. (1991). Corn growth responses to potassium fertilization on three compacted soils. *Soil Till Resources*, 21:287-298.

Zhang, L., & Grift, T. E. (2012). A monocular vision-based diameter sensor for miscanthus giganteus. *Biosystems Engineering*, 111:298-304.

Zia, S., Romano, G., Spreer, W., Shanchez, J., Cairns, J., Araus, L., & Muller, J. (2013). Infrared thermal imaging as rapid tool for identifying water-stress tolerant maize genotypes of different phenology. *Journal of Agronomy and Crop Science*, 199(2):57-84.

APPENDIX

A.1 Matlab® script for diameter acquiring GUI.

 Matlab® scripts were created for image collection and acquisition to determine the diameter of

the stalk of the corn crops. This file can operate in both daylight and night, while saving all

figures for later research purposes in addition to real time readouts.

GUI_CornCane.m

```matlab
function varargout = GUI_CornCane(varargin)

%============================================================
% Author William Edward Roy
% Created March 15 2011
%============================================================

% GUI_CORNCANE M-file for GUI_CornCane.fig
%     GUI_CORNCANE, by itself, creates a new GUI_CORNCANE or raises the existing
%     singleton*.
%
%     H = GUI_CORNCANE returns the handle to a new GUI_CORNCANE or the handle to
%     the existing singleton*.
%
%     GUI_CORNCANE('CALLBACK',hObject,eventData,handles,...) calls the local
%     function named CALLBACK in GUI_CORNCANE.M with the given input arguments.
%
%     GUI_CORNCANE('Property','Value',...) creates a new GUI_CORNCANE or raises the
%     existing singleton*. Starting from the left, property value pairs are
%     applied to the GUI before GUI_CornCane_OpeningFcn gets called. An
%     unrecognized property name or invalid value makes property application
%     stop. All inputs are passed to GUI_CornCane_OpeningFcn via varargin.
%
%     *See GUI Options on GUIDE's Tools menu. Choose "GUI allows only one
%     instance to run (singleton)".
%
% See also: GUIDE, GUIDATA, GUIHANDLES

% Edit the above text to modify the response to help GUI_CornCane
```

```matlab
% Last Modified by GUIDE v2.5 08-Feb-2012 00:59:53

% Begin initialization code - DO NOT EDIT
gui_Singleton = 1;
gui_State = struct('gui_Name',       mfilename, ...
                   'gui_Singleton',  gui_Singleton, ...
                   'gui_OpeningFcn', @GUI_CornCane_OpeningFcn, ...
                   'gui_OutputFcn',  @GUI_CornCane_OutputFcn, ...
                   'gui_LayoutFcn',  [] , ...
                   'gui_Callback',   []);
if nargin && ischar(varargin{1})
   gui_State.gui_Callback = str2func(varargin{1});
end

if nargout
   [varargout{1:nargout}] = gui_mainfcn(gui_State, varargin{:});
else
   gui_mainfcn(gui_State, varargin{:});
end
% End initialization code - DO NOT EDIT


% --- Executes just before GUI_CornCane is made visible.
function GUI_CornCane_OpeningFcn(hObject, eventdata, handles, varargin)
% This function has no output args, see OutputFcn.
% hObject    handle to figure
% eventdata  reserved - to be defined in a future version of MATLAB
% handles    structure with handles and user data (see GUIDATA)
% varargin   command line arguments to GUI_CornCane (see VARARGIN)

% Choose default command line output for GUI_CornCane
handles.output = hObject;

% Update handles structure
guidata(hObject, handles);

% UIWAIT makes GUI_CornCane wait for user response (see UIRESUME)
% uiwait(handles.figure1);


% --- Outputs from this function are returned to the command line.
function varargout = GUI_CornCane_OutputFcn(hObject, eventdata, handles)
% varargout  cell array for returning output args (see VARARGOUT);
% hObject    handle to figure
% eventdata  reserved - to be defined in a future version of MATLAB
% handles    structure with handles and user data (see GUIDATA)
```

```matlab
% Get default command line output from handles structure
varargout{1} = handles.output;


% --- Executes during object creation, after setting all properties.
function popupmenu1_CreateFcn(hObject, eventdata, handles)
% hObject    handle to popupmenu1 (see GCBO)
% eventdata  reserved - to be defined in a future version of MATLAB
% handles    empty - handles not created until after all CreateFcns called

% Hint: popupmenu controls usually have a white background on Windows.
%       See ISPC and COMPUTER.
if ispc && isequal(get(hObject,'BackgroundColor'), get(0,'defaultUicontrolBackgroundColor'))
    set(hObject,'BackgroundColor','white');
end


% --- Executes on button press in Begin_Program.
function Begin_Program_Callback(hObject, eventdata, handles)
clear all
pause on
%=========================== Constants ==============================

map = [(0:1/256:1-1/256)',(0:1/256:1-1/256)',(0:1/256:1-1/256)'];
SwitchThreshold     = 2.5;
ImageThreshold      = 0.80;
% Image size is 800x600
% CCD_Vert_pix        = 600;
% CCD_Hori_pix        = 800;

%======================== Initialization  ==========================

% This translates Vertical Distance in pix to Distance to Stalk in mm
% See File Vert_distanceVSDistanceToStalk.m

a    = 265900;
b    = 1868;   %R Square 0.992

% % This translates Distance to Stalk in mm to mm_per_pixel
% c    = 1.011;
% d    = 27.3;  % deg,

c = 7.2e-004;


%======================== Initialization  ==========================
imaqreset;
```

```matlab
%%===================== camera initialization =========================
Camera = videoinput('dcam', 1,'Y422_800x600');
triggerconfig(Camera, 'manual');
set(Camera,'framespertrigger', 1);
set(Camera,'TriggerRepeat', inf);
set(Camera,'ReturnedColorSpace','RGB')


FileName        = 'Lab_Test'; %input('Enter filename','s');
FilePath        = 'M:\GUI_Test';

K = 1;
i = 1;

%===================== Turn the laser on   =====================
disp('Warming up, please wait, turn on power switch')

while(K ==1 )



  %============================= Aquire image
================================
  start(Camera);
%   pause(0.3);
  trigger(Camera);
  Crescent     = getdata(Camera,1);
  stop(Camera);
%   subplot(1,2,1)
%   imshow(Crescent)
%   imwrite(Crescent,['Crescent2_' num2str(i) '.tif'],'tif');
%

  % ==================== Segment the image
================================

  Crescent_BW      = bwAreaOpen(im2bw(Crescent,ImageThreshold),10);
  [row,col]            = find(Crescent_BW==1);

  nWhite = nnz(Crescent_BW);
   if (nWhite > 500)

  GUI_show = figure;
  subplot(1,2,1)
  imshow(Crescent)
%   imwrite(Crescent,['Crescent2_' num2str(i) '.tif'],'tif');
```

```matlab
  subplot(1,2,2)
  imshow(~Crescent_BW)
%    imwrite(Crescent_BW,['Crescent_BW_' num2str(i) '.tif'],'tif');

  [row,col]       = find(Crescent_BW==1);
  Diameter_pix    = max(col)-min(col)

  line([min(col) min(col)],[min(row) max(row)])
  line([max(col) max(col)],[min(row) max(row)])
  line([min(col) max(col)],[min(row) min(row)])
  line([min(col) max(col)],[max(row) max(row)])

  disp(['Diameter in pixel:' num2str(Diameter_pix)]);

  VertHeight_pix    = min(row)
  disp(['Vertical Height in pixel:' num2str(VertHeight_pix)]);

  % ========= Translate VertHeight_pix into distance to stalk in mm =======

  Dist_stalk_mm    = a./(b-VertHeight_pix)



  mm_pix           = c*Dist_stalk_mm
  StalkDiam        = mm_pix * Diameter_pix
  StalkDiamVec(i)  = StalkDiam;

  text(50,500,['Dist stalk, mm ' num2str(Dist_stalk_mm)])
  text(50,550,['Stalk Diam, mm ' num2str(StalkDiam)])

  ImagData = ScreenCapture(GUI_show);
%    imwrite(Crescent,['Crescent2_' num2str(i) '.tif'],'tif');
%    imwrite(Crescent_BW,['Crescent_BW_' num2str(i) '.tif'],'tif');
  imwrite(uint8(ImagData),['regression_mod4' num2str(i) '.jpg'],'jpg');



  pause(0.5)
  close(GUI_show)
%    clc

  i               = i + 1;
   else
      display('no laser pixel');
end;
end;
```

```matlab
% hObject    handle to Begin_Program (see GCBO)
% eventdata  reserved - to be defined in a future version of MATLAB
% handles    structure with handles and user data (see GUIDATA)


% --- Executes on button press in Exit.
function Exit_Callback(hObject, eventdata, handles)
logo = imread('illini.jpg');
deere = imread('deere.jpg');
% me = imread('Ed.JPG');
subplot(1,2,1);
imshow(logo);
subplot(1,2,2);
imshow(deere);
% subplot(2,2,3);
% imshow(me);
pause(5);
close GUI_CornCane;
exit
% hObject    handle to Exit (see GCBO)
% eventdata  reserved - to be defined in a future version of MATLAB
% handles    structure with handles and user data (see GUIDATA)


% --- Executes on button press in pause_button.
function pause_button_Callback(hObject, eventdata, handles)
pause on
disp 'you have paused the program, press begin to start data collection again';
pause (10000000000000);


% hObject    handle to pause_button (see GCBO)
% eventdata  reserved - to be defined in a future version of MATLAB
% handles    structure with handles and user data (see GUIDATA)


% --- Executes on button press in About_button.
function About_button_Callback(hObject, eventdata, handles)
msgbox('This program is designed to give you the image, measurement, and distance away from
a corn stalk. The end goal is to be able to accurately measure the yield of the corn crop in the
early growth season before the Combine travels through in the later season');

% hObject    handle to About_button (see GCBO)
% eventdata  reserved - to be defined in a future version of MATLAB
% handles    structure with handles and user data (see GUIDATA)
```

```matlab
% --- Executes on button press in preview.
function preview_Callback(hObject, eventdata, handles)
imaqreset;
Camera = videoinput('dcam', 1,'Y422_800x600');
triggerconfig(Camera, 'manual');
set(Camera,'framespertrigger', 1);
set(Camera,'TriggerRepeat', inf);
set(Camera,'ReturnedColorSpace','RGB');
preview(Camera);
pause(10);
open GUI_CornCane;
% hObject    handle to preview (see GCBO)
% eventdata  reserved - to be defined in a future version of MATLAB
% handles    structure with handles and user data (see GUIDATA)


% --- Executes on button press in example_picture.
function example_picture_Callback(hObject, eventdata, handles)
demo = imread('demo.jpg');
imshow(demo);
pause(6);
% hObject    handle to example_picture (see GCBO)
% eventdata  reserved - to be defined in a future version of MATLAB
% handles    structure with handles and user data (see GUIDATA)
```

A.2 Matlab® script for the camera calibration.

These are 2 independent scripts needed to calibrate the cameras to establish the most precise

pixel to millimeter accuracy of each image.

DepthModel.m

```matlab
% Depth Model of height to distance of the laser and camera. Step 1 of
% final calibration. The data points of x and y are representive of
% distance the lasrer moved and distance away from the target board.

%===========================================================
% Author William Edward Roy
% Created July 28 2012
%===========================================================
```

```matlab
%ydata and xdata are measures distance points in mm
ydata = [215 210 205 200 195 190 185 180 175 170 165 160 155 150]
xdata = [600 599 582 547 516 481 445 392 355 301 256 206 139 82]


% Outputs from the toolbox needed
a=265900;
b=1868;   %R Square 0.992

x=82:600;
y=a./(b-x);

% Graph showing that this was all correct
plot(xdata,ydata,'*');hold on;
ylabel('Distance from Stalk mm')
xlabel('Vertical Height of Laser Sheet pixel')
plot(x,y,'-r');grid on;
```

DepthModelpart2.m

```matlab
% Part 2 of the laser depth calibration. We are creating a linear plot to
% demonstraignt the camera distance (datax) and the mm/pixel (ydata)
% solving for b in equation 8 to be 27.3, averaging from the highest and
% lowest values.

%============================================================
% Author William Edward Roy
% Created July 28 2012
%============================================================


datax = [150 155 160 165 170 175 180 185 190 195 200 205 210 215]
datay = [0.08625 0.09125 0.095 0.098125 0.101875 0.10625 0.11 0.113125 ...
    0.1175 0.121875 0.125 0.12875 0.13125 0.136875]

% %R Square 0.9617 variables b and a are aquired by a best fit analysis.
b=27.3;
a=1.011;
datax=150:215;
datay=a.*(2*tand(27.3/2))*(0.00125)*(datax);

plot(datax,datay,'*');hold on;
plot(datax,datay,'-r');grid on;
```

```matlab
xlabel('Distance form Corn Stalk mm')
ylabel('Horizontal Covered Lemgth per Pixel mm/pixel')
% Linear model:
%      f(datax) = a*2*tan(27.3/2)*(0.00125)*(datax)
% Coefficients (with 95% confidence bounds):
%       a =        0.13  (0.1279, 0.1321)
%
% Goodness of fit:
%    SSE: 0.0001258
%    R-square: 0.9617
%    Adjusted R-square: 0.9617
%    RMSE: 0.003111
```

A.3 Matlab® script to acquire the original images used for camera calibration.

image_collection.m

```matlab
% Camera Calibration file needing 25 images to create a Mosaic.
% Turn on camera then hit "enter" for an image and save in tif format in docs.
% =======================Constants/Turn on============================

%==========================================================
% Author William Edward Roy
% Created December 28 2011
%==========================================================

clc
close all
map = [(0:1/256:1-1/256)',(0:1/256:1-1/256)',(0:1/256:1-1/256)'];
rgbmap = ycbcr2rgb(map);

imaqreset;


% ===================== Camera turn on============================
vid1 = videoinput('dcam', 1, 'Y422_800x600');
triggerconfig (vid1, 'manual');
set(vid1,'ReturnedColorSpace','RGB')
set(vid1, 'framespertrigger', 1);
set(vid1,'TriggerRepeat', inf);
filename = 'Calibration';
close all
start(vid1);
```

```matlab
% =====================Take image===============================
for i = 1 : 25 %Take exactly 25 images of the target board at multiple angles
  trigger(vid1);
  Calibration_Image = getdata(vid1,1);
  Calibration_Image = rgb2gray(Calibration_Image);
  % ===================save images===============================
  imwrite(Calibration_Image,[num2str(filename) '_ccl_' num2str(i) '.tif'],'tif');
  pause
  disp(['Hit Enter i= ' num2str(i)])
end
```

A.4 Matlab® script for analyzing the collected data from the greenhouse study.

The script produces a statistical breakdown of the strong correlation between the measured diameter of the stalk by handheld calipers and the measured diameter from the optical camera and laser system. This was to confirm accuracy of the optical platform.

regression_model.m

```matlab
% The goal of this study was to take 126 corn plants diameters in a green
%   house with a pair of normal measuring calipers and then a second time with
%   the optical sensor created by myself. After collecting the data results,
%   a regression was created to varify the correctness of the sensor and justify
%   its creation.

% Author William E Roy Technical Systems Management Masters Student

% datax represents the measurments taken with the HANDHELD calipers

%===========================================================
% Author William Edward Roy
% Created September 1 2012
%===========================================================


datax = [25.54 24.82 25.61 28.09 26.13 25.94 25.85 29.00 25.22 28.96 29.08 ...
         24.22 25.71 25.19 26.02 26.26 26.75 29.34 25.59 25.24 25.76 24.86 ...
         27.91 23.88 26.26 27.85 30.89 25.59 26.18 24.34 26.38 24.39 24.87 ...
         24.77 23.59 17.51 24.62 26.50 26.99 24.33 25.05 29.23 23.87 28.10 ...
         27.75 23.76 26.02 26.64 20.98 22.90 28.38 25.82 23.96 25.65 26.19 ...
         27.60 27.50 23.97 24.92 26.31 29.26 25.89 28.84 25.32 19.97 24.31 ...
```

```
        26.28 30.77 24.67 28.25 27.45 28.87 23.42 24.49 24.75 31.49 31.10 ...
        27.53 24.26 24.12 29.05 30.40 24.15 23.01 23.94 29.14 26.42 24.51 ...
        27.92 29.68 23.22 25.46 27.03 23.65 26.04 27.44 26.33 25.19 25.15 ...
        28.13 27.61 24.31 26.74 26.44 29.75 27.44 18.29 30.49 23.72 25.75 ...
        26.76 19.34 15.82 26.46 26.39 23.06 23.55 26.61 26.24 25.57 29.52 ...
        24.58 27.48 36.30 28.62 26.97];

% datay represents the measurments taken with the OPTICAL sensor

datay = [26.50 25.30 25.47 28.60 27.36 22.60 25.50 29.84 25.58 30.38 29.19 ...
        23.46 22.10 24.39 25.24 26.53 28.68 29.61 21.62 22.98 26.17 24.69 ...
        28.09 25.67 25.25 26.19 31.78 26.70 27.04 25.60 26.82 21.08 24.92 ...
        26.08 24.58 14.00 25.57 27.27 27.09 24.88 25.60 29.16 23.89 28.17 ...
        22.61 23.78 24.64 26.10 21.21 22.47 28.58 25.29 24.52 25.55 26.00 ...
        27.40 27.65 24.77 24.64 27.47 29.45 25.95 28.50 26.28 20.69 26.27 ...
        25.62 30.48 25.51 28.93 24.69 29.05 21.66 23.86 23.43 31.55 30.97 ...
        27.61 25.49 22.80 29.57 30.41 24.02 22.50 24.02 28.32 27.84 25.33 ...
        27.58 29.88 22.26 25.70 26.48 23.96 25.67 26.72 26.77 24.08 25.55 ...
        28.38 28.91 24.78 26.88 26.16 29.21 27.45 18.31 30.46 23.96 25.37 ...
        26.60 15.43 17.28 26.40 25.08 25.05 22.68 25.61 26.41 26.07 29.40 ...
        24.51 25.65 35.67 28.61 25.97];

% figure



    % plot(datax,datay,'*');hold on;

figure
plot(datax,datay,'s','MarkerEdgeColor','k',...
            'MarkerFaceColor','g','MarkerSize',10);hold on;
        set(gca,'Color',[0.5 0.5 0.5])
title('Regression between Hand and Optical Measurements')
xlabel('Hand Diameter Measurements (mm)');
ylabel('Optical Diameter Measurements (mm)');hold on;

% Calculations to establish the R-Squared

p = polyfit(datax,datay,1);
yfit = polyval(p,datax);
yresid = datay - yfit;
SSresid = sum(yresid.^2);
SStotal = (length(datay)-1) * var(datay);
rsq = 1 - SSresid/SStotal;

text(30,20,['R-Squared  ' num2str(rsq)])
```

```matlab
% --- Create fit "fit 1"
ok_ = isfinite(datax) & isfinite(datay);
if ~all( ok_ )
    warning( 'GenerateMFile:IgnoringNansAndInfs', ...
        'Ignoring NaNs and Infs in data' );
end
ft_ = fittype('poly1');

% Fit this model using new data
cf_ = fit(datax(ok_)',datay(ok_)',ft_);

% Or use coefficients from the original fit:
if 0
    cv_ = { 1.0210770999737067, -0.70524707323589653};
    cf_ = cfit(ft_,cv_{:});
end

% Plot this fit with a 95% confidence
h_ = plot(cf_,'fit',0.95);
xlabel('Hand Diameter Measurements (mm)');
ylabel('Optical Diameter Measurements (mm)');

legend ('handheld vs. optical','fitted curve');  % turn off legend from plot method call
set(h_(1),'Color',[1 0 0],...
    'LineStyle','-', 'LineWidth',2,...
    'Marker','none', 'MarkerSize',6);

figure
subplot(1,2,1);
hist(datax,30);
h = findobj(gca,'Type','patch');
set(h,'FaceColor','b','EdgeColor','w');hold on;
title('Histogram of Handheld Measurements (Left)');
xlabel('Measurement (mm)');
ylabel('Frequency');
set(gca,'Color',[0.5 0.5 0.5])

Subplot(1,2,2);
hist(datay,30);
h = findobj(gca,'Type','patch');
set(h,'FaceColor','g','EdgeColor','w');hold on;
title('Histogram of Optical Measurements (Right)');
xlabel('Measurement (mm)');
ylabel('Frequency');
set(gca,'Color',[0.5 0.5 0.5])
```

```matlab
figure
plot(datax,'>','MarkerEdgeColor','k',...
            'MarkerFaceColor','b','MarkerSize',10);hold on;
title('Regression between Hand and Optical Measurements')
xlabel('Total Number of Measurements Taken');
ylabel('Stalk Measurement Values');hold on;

plot(datay,'g*',...
    'MarkerSize',10);
legend('handheld','optical');
text(100,12,['R-Squared  ' num2str(rsq)])
set(gca,'Color',[0.5 0.5 0.5])

figure
subplot(1,2,1);
boxplot(datax,'symbol','b+',...
    'colors','b');%hold on;
title('Boxplot of Handheld Measurments');
xlabel('Number of Measurments');
ylabel('Handheld Diameter Measurement (mm)');
set(gca,'Color',[0.5 0.5 0.5])

subplot(1,2,2);
boxplot(datay,'symbol','g+',...
    'colors','g');
  set(gca,'Color',[0.5 0.5 0.5])

title('Boxplot of Optical Measurments');
xlabel('Number of Measurments');
ylabel('Optical Diameter Measurement (mm)');


% Linear model Poly1:
%      f(x) = p1*x + p2
% Coefficients (with 95% confidence bounds):
%      p1 =      1.021  (0.9414, 1.101)
%      p2 =    -0.7052  (-2.792, 1.381)
%
% Goodness of fit:
%   SSE: 188.2
%   R-square: 0.8384
%   Adjusted R-square: 0.8371
%   RMSE: 1.232
```

stat_analysis2.m

```
% The focus of this study was to determine that regression between the
% total weight of the crop ear (kernels + cob) and the stalk diameter
% If the R^2 proved to be significant enough, one would be able to justify
%that the diameter of the corn stalk can be used as a means of phenotyping
%and yield estimation.

% Author William E Roy Technical Systems Management Masters Student

% datax represents the weight of the corn ear plus kernals in the units of
% grams

datax = [209.20 218.25 226.22 295.02 246.16 245.96 217.10 286.92 277.30 ...
        259.11 160.24 183.08 308.03 191.42 200.61 233.34 272.89 210.22 ...
        179.14 274.95 222.90 227.47 121.16 168.52 190.54 249.92 219.40 ...
        257.19 272.21 263.35 231.62 280.38 218.22 234.13 236.87];

% datay represents the diameter measurements with the optical sensor

datay = [19.58 21.43 22.18 24.39 23.15 20.78 20.67 23.21 25.26 24.01 18.62 ...
        20.99 24.82 21.04 22.21 23.34 22.73 20.85 17.91 24.35 21.67 20.92 ...
        17.34 20.01 21.14 23.09 21.29 23.05 24.88 23.27 23.60 ...
        27.22 22.01 23.13 23.39];

% figure



    % plot(datax,datay,'*');hold on;

% Regression Plot
figure
plot(datax,datay,'s','MarkerEdgeColor','k',...
            'MarkerFaceColor','g','MarkerSize',10);hold on;
        set(gca,'Color',[0.5 0.5 0.5])
title('Regression between Corn Stalk Diameter and Weight of Crop Ear')
xlabel('Weight of Ear with Kernals (g)');
ylabel('Optical Diameter Measurements (mm)');hold on;

% Calculations to establish the R-Squared

p = polyfit(datax,datay,1);
yfit = polyval(p,datax);
yresid = datay - yfit;
SSresid = sum(yresid.^2);
SStotal = (length(datay)-1) * var(datay);
rsq = 1 - SSresid/SStotal;
```

```matlab
text(240,17,['R-Squared  ' num2str(rsq)])


% --- Create fit "fit 1"
ok_ = isfinite(datax) & isfinite(datay);
if ~all( ok_ )
    warning( 'GenerateMFile:IgnoringNansAndInfs', ...
        'Ignoring NaNs and Infs in data' );
end
ft_ = fittype('poly1');

% Fit this model using new data
cf_ = fit(datax(ok_)',datay(ok_)',ft_);

% Or use coefficients from the original fit:
if 0
    cv_ = { 1.0210770999737067, -0.70524707323589653};
    cf_ = cfit(ft_,cv_{:});
end

% Plot this fit with a 95% confidence
h_ = plot(cf_,'fit',0.95);
xlabel('Weight of Ear with Kernals (g)');
ylabel('Optical Diameter Measurements (mm)');

legend ('diameter vs. ear weight','fitted curve');  % turn off legend from plot method call
set(h_(1),'Color',[1 0 0],...
    'LineStyle','-', 'LineWidth',2,...
    'Marker','none', 'MarkerSize',6);

% Historgam
figure
subplot(1,2,1);
hist(datax,30);
h = findobj(gca,'Type','patch');
set(h,'FaceColor','b','EdgeColor','w');hold on;
title('Histogram of Ear Weight (Left)');
xlabel('Measurement (g)');
ylabel('Frequency');
set(gca,'Color',[0.5 0.5 0.5])

Subplot(1,2,2);
hist(datay,30);
h = findobj(gca,'Type','patch');
set(h,'FaceColor','g','EdgeColor','w');hold on;
```

```matlab
title('Histogram of Optical Measurements (Right)');
xlabel('Measurement (mm)');
ylabel('Frequency');
set(gca,'Color',[0.5 0.5 0.5])

% Boxplot
figure
subplot(1,2,1);
boxplot(datax,'symbol','b+',...
    'colors','b');%hold on;
title('Boxplot of Ear Weight Measurements');
xlabel('Number of Measurments');
ylabel('Ear Weight Measurements (g)');
set(gca,'Color',[0.5 0.5 0.5])

subplot(1,2,2);
boxplot(datay,'symbol','g+',...
    'colors','g');
  set(gca,'Color',[0.5 0.5 0.5])

title('Boxplot of Optical Measurments');
xlabel('Number of Measurments');
ylabel('Optical Diameter Measurement (mm)');
```

stat_analysis3.m

```matlab
% The focus of this study was to determine that regression between the
% total weight of the crop ear kernels only. If the R^2 proved to be
% significant enough, one would be able to justify that the diameter of the
% corn stalk can be used as a means of phenotyping and yield estimation.


% Author William E Roy Technical Systems Management Masters Student

% datax represents the weight of the kernals in the units of
% grams

datax = [189.14 198.41 203.47 254.84 220.38 224.94 198.97 260.53 246.33 ...
    234.49 145.48 162.44 275.25 176.81 179.97 211.24 235.54 ...
    193.17 158.56 250.72 204.24 207.04 110.27 154.06 171.88 224.36 ...
    198.49 230.24 242.34 238.45 211.53 260.32 187.91 209.66 215.30];

% datay represents the diameter measurements with the optical sensor

datay = [19.58 21.43 22.18 24.39 23.15 20.78 20.67 23.21 25.26 24.01 18.62 ...
```

```matlab
                20.99 24.82 21.04 22.21 23.34 22.73 20.85 17.91 24.35 21.67 20.92 ...
                17.34 20.01 21.14 23.09 21.29 23.05 24.88 23.27 23.60 ...
                27.22 22.01 23.13 23.39];

% figure



    % plot(datax,datay,'*');hold on;

% Regression Plot
figure
plot(datax,datay,'s','MarkerEdgeColor','k',...
            'MarkerFaceColor','g','MarkerSize',10);hold on;
        set(gca,'Color',[0.5 0.5 0.5])
title('Regression between Corn Stalk Diameter and Weight of Crop Ear Kernels Only')
xlabel('Weight of Kernals (g)');
ylabel('Optical Diameter Measurements (mm)');hold on;

% Calculations to establish the R-Squared

p = polyfit(datax,datay,1);
yfit = polyval(p,datax);
yresid = datay - yfit;
SSresid = sum(yresid.^2);
SStotal = (length(datay)-1) * var(datay);
rsq = 1 - SSresid/SStotal;

text(220,17,['R-Squared  ' num2str(rsq)])


% --- Create fit "fit 1"
ok_ = isfinite(datax) & isfinite(datay);
if ~all( ok_ )
   warning( 'GenerateMFile:IgnoringNansAndInfs', ...
      'Ignoring NaNs and Infs in data' );
end
ft_ = fittype('poly1');

% Fit this model using new data
cf_ = fit(datax(ok_)',datay(ok_)',ft_);

% Or use coefficients from the original fit:
if 0
   cv_ = { 1.0210770999737067, -0.70524707323589653};
   cf_ = cfit(ft_,cv_{:});
```

```matlab
end

% Plot this fit with a 95% confidence
h_ = plot(cf_,'fit',0.95);
xlabel('Total Weight of Kernels only (g)');
ylabel('Optical Diameter Measurements (mm)');

legend ('diameter vs. kernel weight','fitted curve');  % turn off legend from plot method call
set(h_(1),'Color',[1 0 0],...
    'LineStyle','-', 'LineWidth',2,...
    'Marker','none', 'MarkerSize',6);

% Historgam
figure
subplot(1,2,1);
hist(datax,30);
h = findobj(gca,'Type','patch');
set(h,'FaceColor','b','EdgeColor','w');hold on;
title('Histogram of Kernel Weight (Left)');
xlabel('Measurement (g)');
ylabel('Frequency');
set(gca,'Color',[0.5 0.5 0.5])

Subplot(1,2,2);
hist(datay,30);
h = findobj(gca,'Type','patch');
set(h,'FaceColor','g','EdgeColor','w');hold on;
title('Histogram of Optical Measurements (Right)');
xlabel('Measurement (mm)');
ylabel('Frequency');
set(gca,'Color',[0.5 0.5 0.5])

% Boxplot
figure
subplot(1,2,1);
boxplot(datax,'symbol','b+',...
    'colors','b');%hold on;
title('Boxplot Total Weight of Kernels only');
xlabel('Number of Measurments');
ylabel('Ear Weight Measurements (g)');
set(gca,'Color',[0.5 0.5 0.5])

subplot(1,2,2);
boxplot(datay,'symbol','g+',...
    'colors','g');
    set(gca,'Color',[0.5 0.5 0.5])
```

```matlab
title('Boxplot of Optical Measurments');
xlabel('Number of Measurments');
ylabel('Optical Diameter Measurement (mm)');
```

stat_analysis4.m

```matlab
% The focus of this study was to determine the regression between the
% total weight of the crop ear kernels only and number of kernels per ear.
% If the R^2 proved to be significant enough, one would be able to justify that the diameter of the
% corn stalk can be used as a means of phenotyping and yield estimation.


% Author William E Roy Technical Systems Management Masters Student

% datax represents the weight of the kernals in the units of
% grams

datax = [189.14 198.41 203.47 254.84 220.38 224.94 198.97 260.53 246.33 ...
    234.49 145.48 162.44 275.25 176.81 179.97 211.24 235.54 ...
    193.17 158.56 250.72 204.24 207.04 110.27 154.06 171.88 224.36 ...
    198.49 230.24 242.34 238.45 211.53 260.32 187.91 209.66 215.30];

% datay represents the counted number of kernels per ear.

datay = [420 464 449 607 553 532 440 562 590 570 338 390 599 429 360 455 ...
    548 464 366 572 466 490 411 401 391 529 544 499 508 535 520 643 ...
    384 447 497];

% figure



    % plot(datax,datay,'*');hold on;

% Regression Plot
figure
plot(datax,datay,'s','MarkerEdgeColor','k',...
        'MarkerFaceColor','g','MarkerSize',10);hold on;
    set(gca,'Color',[0.5 0.5 0.5])
title('Regression between Total Weight of Corn Kernels and Number of Kernels per Ear')
xlabel('Weight of Ear with Kernals only (g)');
ylabel('Number of Kernels per Ear');hold on;

% Calculations to establish the R-Squared
```

```matlab
p = polyfit(datax,datay,1);
yfit = polyval(p,datax);
yresid = datay - yfit;
SSresid = sum(yresid.^2);
SStotal = (length(datay)-1) * var(datay);
rsq = 1 - SSresid/SStotal;

text(220,300,['R-Squared  ' num2str(rsq)])


% --- Create fit "fit 1"
ok_ = isfinite(datax) & isfinite(datay);
if ~all( ok_ )
    warning( 'GenerateMFile:IgnoringNansAndInfs', ...
        'Ignoring NaNs and Infs in data' );
end
ft_ = fittype('poly1');

% Fit this model using new data
cf_ = fit(datax(ok_)',datay(ok_)',ft_);

% Or use coefficients from the original fit:
if 0
    cv_ = { 1.0210770999737067, -0.70524707323589653};
    cf_ = cfit(ft_,cv_{:});
end

% Plot this fit with a 95% confidence
h_ = plot(cf_,'fit',0.95);
xlabel('Total Weight of Kernels only (g)');
ylabel('Number of Kernels per Ear');

legend ('Kernel Weight vs Kernel Count','fitted curve');  % turn off legend from plot method call
set(h_(1),'Color',[1 0 0],...
    'LineStyle','-', 'LineWidth',2,...
    'Marker','none', 'MarkerSize',6);

% Historgam
figure
subplot(1,2,1);
hist(datax,30);
h = findobj(gca,'Type','patch');
set(h,'FaceColor','b','EdgeColor','w');hold on;
title('Histogram of Total Weight of Kernels only (Left)');
xlabel('Measurement (g)');
```

```matlab
ylabel('Frequency');
set(gca,'Color',[0.5 0.5 0.5])

Subplot(1,2,2);
hist(datay,30);
h = findobj(gca,'Type','patch');
set(h,'FaceColor','g','EdgeColor','w');hold on;
title('Histogram of Number of Kernels per Ear (Right)');
xlabel('population');
ylabel('Frequency');
set(gca,'Color',[0.5 0.5 0.5])

% Boxplot
figure
subplot(1,2,1);
boxplot(datax,'symbol','b+',...
    'colors','b');%hold on;
title('Boxplot Total Weight of Kernels only (g)');
xlabel('Number of Measurments');
ylabel('Ear Weight Measurements (g)');
set(gca,'Color',[0.5 0.5 0.5])

subplot(1,2,2);
boxplot(datay,'symbol','g+',...
    'colors','g');
  set(gca,'Color',[0.5 0.5 0.5])

title('Boxplot of Number of Kernels per Ear');
xlabel('Number of Measurments');
ylabel('Number of Kernels per Ear');
```

stat_analysis5.m

```matlab
% The focus of this study was to determine that regression between the
% stalk diameter and number of kernals per ear
% If the R^2 proved to be significant enough, one would be able to justify that the diameter of the
% corn stalk can be used as a means of phenotyping and yield estimation.

% Author William E Roy Technical Systems Management Masters Student

% datax represents the counted number of kernels per ear.

datax = [420 464 449 607 553 532 440 562 590 570 338 390 599 429 360 455 ...
    548 464 366 572 466 490 411 401 391 529 544 499 508 535 520 643 ...
    384 447 497];
```

```matlab
% datay represents the diameter measurements with the optical sensor

datay = [19.58 21.43 22.18 24.39 23.15 20.78 20.67 23.21 25.26 24.01 18.62 ...
    20.99 24.82 21.04 22.21 23.34 22.73 20.85 17.91 24.35 21.67 20.92 ...
    17.34 20.01 21.14 23.09 21.29 23.05 24.88 23.27 23.60 ...
    27.22 22.01 23.13 23.39];

% figure



  % plot(datax,datay,'*');hold on;

% Regression Plot
figure
plot(datax,datay,'s','MarkerEdgeColor','k',...
        'MarkerFaceColor','g','MarkerSize',10);hold on;
    set(gca,'Color',[0.5 0.5 0.5])
title('Regression between Corn Stalk Diameter and Number of Kernels per Ear')
xlabel('Number of Kernels per Ear');
ylabel('Optical Diameter Measurements (mm)');hold on;

% Calculations to establish the R-Squared

p = polyfit(datax,datay,1);
yfit = polyval(p,datax);
yresid = datay - yfit;
SSresid = sum(yresid.^2);
SStotal = (length(datay)-1) * var(datay);
rsq = 1 - SSresid/SStotal;

text(500,17,['R-Squared  ' num2str(rsq)])


% --- Create fit "fit 1"
ok_ = isfinite(datax) & isfinite(datay);
if ~all( ok_ )
   warning( 'GenerateMFile:IgnoringNansAndInfs', ...
      'Ignoring NaNs and Infs in data' );
end
ft_ = fittype('poly1');

% Fit this model using new data
cf_ = fit(datax(ok_)',datay(ok_)',ft_);
```

```matlab
% Or use coefficients from the original fit:
if 0
    cv_ = { 1.0210770999737067, -0.70524707323589653};
    cf_ = cfit(ft_,cv_{:});
end

% Plot this fit with a 95% confidence
h_ = plot(cf_,'fit',0.95);
xlabel('Number of Kernels per Ear');
ylabel('Optical Diameter Measurements (mm)');

legend ('Diameter vs. Kernels per Ear','fitted curve');  % turn off legend from plot method call
set(h_(1),'Color',[1 0 0],...
    'LineStyle','-', 'LineWidth',2,...
    'Marker','none', 'MarkerSize',6);

% Historgam
figure
subplot(1,2,1);
hist(datax,30);
h = findobj(gca,'Type','patch');
set(h,'FaceColor','b','EdgeColor','w');hold on;
title('Histogram of Kernel count per Ear (Left)');
xlabel('Number of Kernels');
ylabel('Frequency');
set(gca,'Color',[0.5 0.5 0.5])

Subplot(1,2,2);
hist(datay,30);
h = findobj(gca,'Type','patch');
set(h,'FaceColor','g','EdgeColor','w');hold on;
title('Histogram of Optical Measurements (Right)');
xlabel('Measurement (mm)');
ylabel('Frequency');
set(gca,'Color',[0.5 0.5 0.5])

% Boxplot
figure
subplot(1,2,1);
boxplot(datax,'symbol','b+',...
    'colors','b');%hold on;
title('Boxplot of Kernels per Ear');
xlabel('Number of Measurments');
ylabel('Kernels per Ear');
set(gca,'Color',[0.5 0.5 0.5])
```

```matlab
subplot(1,2,2);
boxplot(datay,'symbol','g+',...
    'colors','g');
  set(gca,'Color',[0.5 0.5 0.5])

title('Boxplot of Optical Measurments');
xlabel('Number of Measurments');
ylabel('Optical Diameter Measurement (mm)');
```

A.5 Matlab® script for Rhizotron image acquisition

```matlab
clear all;
close all;
clc;


SplitFactor        = 2;

Intensity_Adjust    = -80;


RhizoImage         = imread('image_name.jpg');

imshow(RhizoImage)

RhizoImage         = RhizoImage + Intensity_Adjust;

RhizoImage         = RhizoImage(:,:,3); % Blue component

figure,imshow(RhizoImage)

RhizoImage_bw      = im2bw(RhizoImage);

Rhizo_conn         = bwlabel(RhizoImage_bw, 8); % 8-connectivity

figure,imshow(RhizoImage_bw)

RhizoImage_open     = bwareaopen(RhizoImage_bw,500);

Rhizo_Properties    = regionprops(RhizoImage_open, 'all');
Rhizo_Area         = [Rhizo_Properties.Area]';
Rhizo_Centroid      = [Rhizo_Properties.Centroid]';
Rhizo_Bounding      = [Rhizo_Properties.BoundingBox]'
```

figure,imshow(RhizoImage_open)

A.6 Matlab® script for Rhizotron operations


```
% William Roy
% March 4th 2013
clear all;
close all;
clc;

NrPulses        = 75  ; % II100 -> 90 degrees, II200 -> 180 degrees
Delay           = 2;

%=====================    start feed         ======================
SerialPort = serial('COM3'); % CHECK IN CONTROL PANEL
set(SerialPort,'Baudrate', 9600);
set(SerialPort,'Databits', 8);
set(SerialPort,'Parity','none');
set(SerialPort,'StopBits', 1);
set(SerialPort,'Terminator','CR');

fopen(SerialPort);

fprintf(SerialPort,'SP')     % Power on to hold camera cart
fprintf(SerialPort,'CR')
% %
fprintf(SerialPort,'SH')     % Half step
fprintf(SerialPort,'CR')
%
fprintf(SerialPort,'BD1')    % Board select is 1
fprintf(SerialPort,'CR')
%
% % fprintf(SerialPort,'SF')
% % fprintf(SerialPort,'CR')
% %
% % fprintf(SerialPort,'SP')
% % fprintf(SerialPort,'CR')
%
% fprintf(SerialPort,'SD2000')     % Set step delay to 800 us
% fprintf(SerialPort,'CR')

% Select Pin 8 from STP101 board
fprintf(SerialPort,'PC8')
```

```matlab
% Send +5 volt signal to noid to activate camera
disp('off')for i = 1:100
   pause
fprintf(SerialPort,'BD1')
fprintf(SerialPort,'PS8')
disp('on')

for k = 1 : 1
%    ============================   Turn
%============================
    fprintf(SerialPort,['II' num2str(NrPulses )]')
    fprintf(SerialPort,'CR');
    pause(Delay)

end
fclose(SerialPort);
```